sustainability

MDPI

Article

Evaluation of Bioenergy Potential and Relative Impact of Microclimate Conditions for Sustainable Fuel Pellets Production and Carbon Sequestration of Short-Rotation Forestry (*Populus* × *Canadensis* Moench.) in Reclaimed Land, South Korea: Three-Year Monitoring

Jihwi Jang [1], Su Young Woo [2,*], Myeong Ja Kwak [2], Sun Mi Je [3], Jong Kyu Lee [2] and Ie Reh Kim [2]

1 New Zealand School of Forestry, University of Canterbury, Christchurch 8140, New Zealand; jangjihwi@naver.com
2 Department of Environmental Horticulture, University of Seoul, Seoul 02504, Korea; 016na8349@hanmail.net (M.J.K.); gpl90@naver.com (J.K.L.); abqlfk@naver.com (I.R.K.)
3 Urban Forests Research Center, National Institute of Forest Science, Seoul 02455, Korea; jesm0211@korea.kr
* Correspondence: wsy@uos.ac.kr; Tel.: +82-2-6490-2691

Received: 22 June 2020; Accepted: 23 July 2020; Published: 3 August 2020

Abstract: It is important to manage sustainable short-rotation coppices (SRCs), having an important role in carbon sink and bioenergy output, because most of SRCs in South Korea were established on reclaimed land. However, during the last three years, the growth pattern of the SRCs was remarkably changed with soil condition. This study aimed to identify the sustainability of SRCs used for carbon storage, biomass and fuel pellet production, monitoring the neighboring vegetation of SRCs by land-use exchange, examine physiological changes of poplar in a seasonal trend, and to evaluate whether poplar is suitable for making wood pellets over time. The calculated biomass yield per area of poplar grown was 103.07 Mg per total area (55.6 ha), and volumes of carbon dioxide absorption were estimated to be 329.72 Mg CO_2. Wood pellet quality based on the criteria scored third grade, indicating that poplar is appropriate to be manufactured as fuel pellets. Moreover, monitoring of the flora distribution in SRCs revealed changes in species composition. As halophyte was increased during drought, soil organic matter, net growth and total chlorophyll of poplar were significantly decreased. These findings indicate that physiological changes and growth pattern of SRCs may be negatively affected by microclimate and provide better understanding for the effective management of SRCs amid environmental changes.

Keywords: biomass yield; carbon storage; growth pattern; poplar; short-rotation coppices; seasonal trends

1. Introduction

Soaring energy consumption, increasing greenhouse gas (GHG) emissions, and concerns over energy import dependence are prompting global changes in the sources from which energy is expected to be derived in the coming years [1,2]. In South Korea, adoption of the renewable energy portfolio standard (RPS) started in 2015 (3.5%) and has been increasingly adopted since 2017 (5%) and has been estimated to increase by 10% in 2022. Moreover, the Korea Emissions Trading Scheme (K-ETS) was formally launched in January 2015, aiming for a 30% reduction in South Korea's carbon emissions by

2030 from the business-as-usual levels [3]. Moreover, based on the Paris Agreement adopted at the Conference of the Parties 21 (COP 21) of the United Nations Framework Convention on Climate Change (UNFCCC) in 2016, new climate regime (Post-2020), the advanced and developing countries, including South Korea, agreed to work together on GHG reduction, and its technological development was launched. So, the roadmap for reducing GHGs was clarified based on the Paris Agreement. In the case of South Korea, the long-term plan for reducing GHGs was set up to achieve a 37% reduction compared to the emission target of 2030, which is the Intended Nationally Determined Contribution (INDC).

The production of bioenergy in the form of wood pellets was increased in South Korea because wood pellets were shown to be a renewable energy source [4]. Lee and Kang [5] reported the effectivity of GHG reduction using biofuel via forest resources. The substitution and enhancement effect of switching from Bunker-C oil to woody biomass fuels (wood pellets and chips) reduced GHG emissions (1.04 kg CO_2 USD^{-1} $year^{-1}$ when converting to pellets and 1.16 kg CO_2 USD^{-1} $year^{-1}$ when converting to wood chips). When switching from kerosene to woody biomass fuel, the GHG reduction effect is 0.53 kg CO_2 USD^{-1} $year^{-1}$ when converting to pellets and 0.54 kg CO_2 USD^{-1} $year^{-1}$ when converting to wood chips; thus, the effect of converting to wood chips appears to be slightly higher than that of converting to pellets [5] (Table 1). The short-rotation coppice (SRC) method of cultivating poplar (1 to 5 year rotation) in plantation is a successful method for growing large amounts of biomass in a short period on plantations [6–11]. Therefore, Korea Forest Service established "Development planning for SRC culture in Saemangeum reclaimed land" for biomass production and as a solution for the limited land area available for plantations in the Korean peninsula [12], and launched afforestation project in 2012 [13] in Gimje city (Figure 1). It is quite obvious that wood pellets are a renewable energy source since they are made from wood; e.g., refer to biofuel from woody biomass directly, generating heat energy [14]. Moreover, poplar is generally known as a suitable material for SRC planning for several reasons: (1) it can easily adapt to new environments, (2) it is characteristically fast growing, (3) with its wide rhizosphere and high transpiration capacity, it can cleanse the land from fertilizer contamination [15], and (4) its burgeoning rootlet development is favorable for absorbing moisture and nutrients [16]. Saemangeum area, our study site, has the longest sea dike (33.9 km) and is one of the largest reclaimed areas (8,570 ha) in the world [13]. In 1991, a great project commenced in the western coast of South Korea, never tried in the world history, was launched, constructing an embankment for blocking water and inside development will be ongoing till 2020 [13,17].

Table 1. Greenhouse gas (GHG) reduction effectiveness in fuel switching from Bunker-C oil and kerosene to wood biomass [5].

GHG [1] Reduction Project (Boiler Fuel Switching)	Investment Cost (Million USD [2])	Annual GHG Reductions (Mg CO_2 $Year^{-1}$)	Annual GHG Reduction Effect (kg CO_2 USD^{-1} $Year^{-1}$)	Annual Total Profit (Million USD $Year^{-1}$)
From B-C oil to Wood pellet	6.41	6,702	0.14	10.06
From B-C oil to Wood chip	9.12	10,604	0.16	20.9
Sum	15.54	17,306	0.30	30.96
From Kerosene to Wood pellet	1.11	595	0.53	1.78
From Kerosene to Wood chip	13.15	7,071	0.54	27.29
Sum	14.26	7,666	1.07	29.07

[1] GHGs, greenhouse gases; [2] USD, United States dollar.

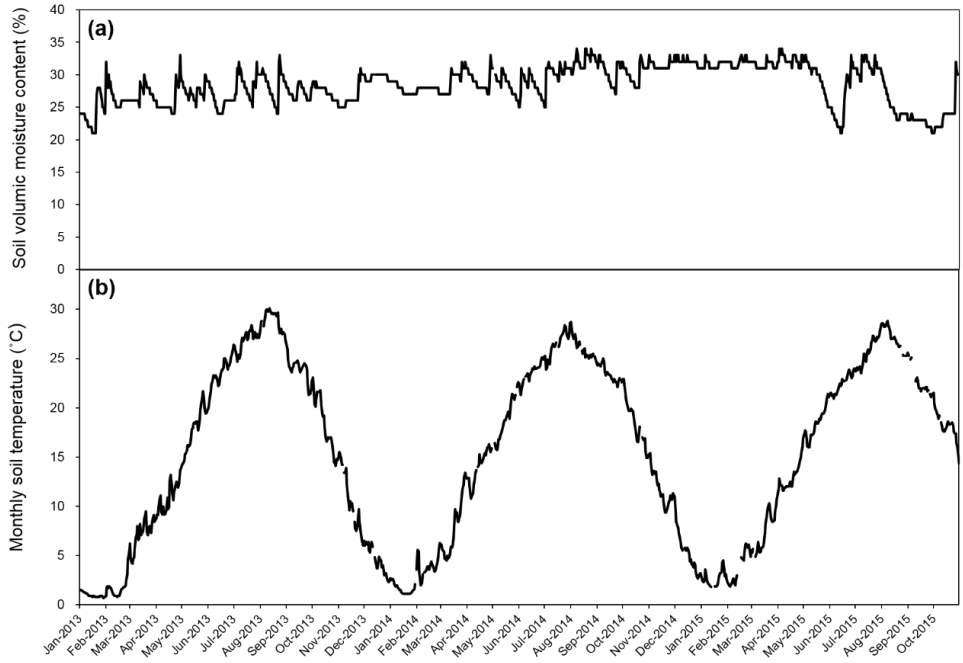

Figure 1. Weather condition of short rotation coppice in Saemangeum reclaimed land, South Korea. (**a**) Soil volumetric moisture content at 30 cm below; (**b**) soil temperature at 30 cm below for the study site throughout 2013, 2014 and 2015.

However, drought is a major environmental constraint on forest productivity [18], and South Korea is no exception. Korea is experiencing a rapid rise in temperature relative to other regions. The average annual temperature in South Korea has risen by 1.2 °C over the past 30 years, which means a faster trend of temperature increase than other regions [19]. Many environmental stresses negatively impact the growth and development of plants, and thereby affect the quantity and quality of crops produced. Drought is one of the most important environmental stresses that alter plant water status [20] and severely limit plant growth and development, as well as high salinity on reclaimed land [21,22]. Woody crops alter their use and allocation of nutrients in response to drought, and changes in soil nutrient cycling and trace gas flux (N_2O and CH_4) are observed when experimental drought is imposed on forests [23]. In our meteorological monitoring in the last three years after afforestation, the Saemangeum reclaimed land had harsh summer conditions with minimal soil moisture, high temperature, high incoming solar radiation and little precipitation, especially in 2015. In general, the surrounding ocean exerts a strong maritime influence, and rainfall is highly regional [24,25], so periods of widely distributed low rainfall are unusual in the climatic record and it might be influenced by high atmospheric pressure from the mainland of China [26]. However, reclaimed land usually has problems related to with temporary drought and fertility, even if the land is in a coastal reclaimed area, such as the western coastal area nearby the Yellow Sea in South Korea [17]. In addition, there was a nationwide drought due to a blocking high-pressure system preventing rainfall across the country, leading to the worst drought since the 1945–1946 season in the past few years, especially in 2013 and 2014 in the Asia-Pacific region [25,27,28], and South Korea was no exception regarding unusual drought conditions, which means a period of sustained dry weather during the summer (November to October) of 2014–2015 [19]. In terms of meteorological monitoring, drought can be defined as a soil moisture deficit caused by insufficient rainfall [29]. Even if the reclaimed land contained high levels of soluble salts and exchangeable sodium that hindered plant growth and reduced fertility during the early stage of reclamation project [30], the pedospeheric condition there was purified through a desalinization process, such as abundant rain or mixing soils and fast-growing tree plantation [13,31]. However, during recent droughts and heat waves in this site, resalinization was temporarily raised as a major environmental stress on the growth and development of woody plants.

The study of stress response in tree species such as poplar is important because of their long-life and their ability to absorb problematic ions, adapting to environmental stress [18]. For these reasons, it is also required to monitor the pedoecological changes and soil nutrient in the Saemangeum area of South Korea and to evaluate how the reclaimed land forestry is affected by microclimate, influencing bioenergy production and sustainability.

Given the importance of biomass production and the sustainable management of SRC in Saemangeum area, the biggest afforested area for producing biomass in South Korea, even in harsh climatic conditions, the aims of this study were (1) to estimate biomass production and carbon storage in SRCs, (2) to evaluate wood pellet quality and the suitability of dry mass yield of poplar trees grown in SRCs, and (3) to determine how changing land use, such as the establishment of SRCs, affects flora distribution in the neighboring vegetation in radically changed pedospheric and meteorological conditions. We explored variation in soil conditions in different SRC types and meteorological conditions in wet (moderate) and drought (temporary drought) years across the annual cycle for three years and identified annual biomass yield and wood pellet productivity in environment variable for sustainable SRC management.

2. Materials and Methods

2.1. Site Description and Microclimate

To embark on an afforestation work for the domestic production of bioenergy and SRC business undertaking, Korea Forest Service leased a piece (506 ha) of Saemangeum reclaimed land (8,570 ha), in a designated area for land substitution (1,000 ha), which mostly composed of dredged soil with mountain soil (0–30%) and sawdust fertilizer (0–6%) [32], on moderate terms from Saemangeum Development and Investment Agency, Sejong city, Korea [13,17]. The University of Seoul research team obtained some study plots in this area (55.6 ha) to monitor forest production and ecophysiological changes for 3 to 4 years. On our site, *Populus* × *Canadensis* Moench. seedlings (2-year-old) were grown for the production of biomass (for 1–3 years) in a designated area on reclaimed land. The total afforested area (SRC) in this site is 55.6 ha, and the estimated total number of planted poplar seedlings in our study site is 343,000 seedlings. Our study site was divided into three types according to being afforested each year over time (2012, 2013 and 2014). Afforestation was conducted in 2012 (2.3 ha; 1 m × 1 m planting interval; 16 plots (5 m × 5 m spacing per plot) per area), 2013 (19.0 ha; 1 m × 1 m planting interval; 12 plots (5 m × 5 m spacing per plot) per area) and 2014 (34.3 ha; 1 m × 1 m planting interval; 12 plots (5 m × 5 m spacing per plot) per area), respectively. In each afforestation site, un-rooted 1 m-long poplar cuttings were planted manually at a density of 10,000 ha^{-1} (1 m × 1 m spacing), among which 1000 seedlings (25 seedlings × 40 plots) were chosen for this study. The experimental site was selected based on biomass yield for producing wood pellets and was situated in the SRC culture on reclaimed land that is part of the marginal lands in the Saemangeum land reclamation project area in Gimje City, Jeollabuk-do Province in Korea at 35°52′ N and 126°47′ E (see Appendix A).

At this site, based on our measurement, the annual rainfall and mean air temperature are approximately 91.28 mm and 13 °C (maximum: 32 °C, minimum −7 °C), respectively, and rainfall is summer dominant; however, summer rainfall in 2015 was much lower than in other periods (see Appendix B). The monthly rainfall from April to October (generally known as the growing season in the southern province of South Korea) in 2013 was 30.21 mm. The precipitation had a marked seasonal concentration in July (accumulated precipitation 333.5 mm). The next year, monthly precipitation from April to October 2014 was 26.84 mm, showing seasonal concentration in August (accumulated precipitation 351.0 mm). The maximum rainfall period was from 10th July to 10th August. During the last year of the experiment (2015), precipitation at this site was affected by drought (rainfall declined by 39.29% and 31.66% in 2015 compared with that of 2013 and 2014, respectively). The monthly precipitation from April to October 2015 was 18.34 mm (accumulated precipitation during the rainy season was 86.5–127.0 mm).

Relative humidity (RH) and air temperature in this study site were monitored and logged automatically from June to October 2015 using one HOBO pro RH/Temp Data loggers and External temp Data Loggers (On-set computer Co., Porasset, MA, USA). The data recordings were taken at one-hour intervals. The other meteorological data in experimental plot were collected from January 2013 to October 2015 by Korea Meteorological Administration (KMA), National climate data service system (see Appendix C). The collected data from KMA were as follows: (1) monthly precipitation, (2) monthly mean temperature, (3) monthly maximum temperature, (4) monthly minimum temperature, and (5) global radiation.

In terms of energy balance, global radiation, including solar radiation, is one of the essential environmental factors which controls both photosynthesis and evapotranspiration, providing the heat, light, and energy necessary for all living organisms, and is consequently an important microclimate variable for microsite study in forestry and environmental science. The global radiation was converted into a photosynthetic photon flux density (PPFD, μmol m^{-2} s^{-1}) using the conversion factor (2.2359) based on the following equation [33], and PPFD was calculated using the method of Suh [33] (see Appendix D). At this site, global radiation and mean photosynthetic photon flux density are approximately 19.3 MJ m^{-2} d^{-1} and 498.3 μmol m^{-2} s^{-1} (maximum: 983.4 μmol m^{-2} s^{-1}, minimum 17.9 μmol m^{-2} s^{-1}), respectively. The photon flux density was determined using the following formula (Equation (1)):

$$PPFD = 2.2359 \times I \ (r = 0.9948) \quad (1)$$

where PPFD is the photosynthetic photon flux density, and I is the global radiation.

2.2. Biomass and Carbon Estimation

Italian poplar (*Populus* × *Canadensis* Moench.), which is known to be suitable for reclaimed land in South Korea [34], was used in this study and was planted on site in 2012, 2013 and 2014 (planting interval, 1 m × 1 m), respectively. To estimate the biomass yield of poplar, we measured the diameter at breast height (DBH) of trees in sample plots in the area (total 40 plots in whole sites; 16 plots in site 2012, 12 plots in site 2013, 12 plots in site 2014) and classified DBH values as minimum, median, and maximum to represent all diameter classes. The biomass yield was determined by cutting down entire trees in the sample plot with a saw 5 cm above the ground by hand saw. A total of 80 trees at each of the different sites (site 2012, 2013 and 2014) were harvested with leaves for the calculation of the aboveground biomass yield during the autumn season, and were separated into stems, branches and leaves. Aboveground samples obtained from every plot were weighed with an electronic scale with an accuracy of 0.1 kg to determine the fresh biomass yield on each plot, and the fresh weight of each sample (stem, branch and leaf) was measured soon after harvesting (data not shown). Poplar trees in the sample plots were subsequently harvested in October 2013, 2014 and 2015, respectively, and oven-dried to a constant weight (oven DS-80-2, Dasol Science, Hwaseong, Korea) at 70 °C for 96 h; the dry weight of the leaves, stems, and branches was then measured [35]. Total biomass (oven-dried tonnes, ODT) was obtained based on these data according to the formula on the estimation of aboveground biomass (Equation (2)), where A and B are coefficients of the regression parameter to be determined, D is the DBH (mm) and ODT is the dry weight of the aboveground mass (Mg ha^{-1} y^{-1}). Stem, branch, and leaf biomass was obtained based on these data, and root biomass was calculated by the method of Caims et al. [36] and Noh et al. [37] (the root biomass is 35% (carbon fraction) of the biomass aboveground). The coefficient estimation method was based on biomass data collected in October 2013, 2014 and 2015, respectively. The root biomass was determined using the following formula (Equation (3)):

$$\mathrm{ODT} = \mathrm{A} \times e^{\mathrm{BD}} \quad (2)$$

$$\text{Root biomass (Mg)} = \mathrm{S} + \mathrm{B} + \mathrm{L} \times 0.35 \quad (3)$$

where A and B are coefficients of the regression parameter to be determined, ODT is the dry weight of aboveground biomass of poplar trees, D is the diameter at breast height, S is the dry weight of the poplar stem, B is the dry weight of the poplar branch, and L is the dry weight the poplar leaf.

To estimate the total biomass production of poplar, the relationship between DBH and dry mass was established (Table 2), and the following formula was applied to calculate the total biomass per area: sum of trees in plot (5 m × 5 m) × 10^4 × (number of trees) $^{-1}$ × 10^{-3}.

Table 2. The coefficient of estimated equation for biomass produced in short-rotation coppices in Saemangeum reclaimed land.

RT *	Part of Tree	A	B	r^2
2013 (13W)	Stem	75.365	0.0796	0.87
	Branch	6.8379	0.1173	0.8167
	Leaf	4.8937	0.0865	0.89
	Root		(aboveground biomass [1]) × 0.35 [a]	
RT	**Part of Tree**	**A**	**B**	**r^2**
2014 (14W)	Stem	58.951	0.0753	0.93
	Branch	8.8832	0.0836	0.89
	Leaf	4.148	0.0768	0.93
	Root		(aboveground biomass [1]) × 0.35 [a]	
RT	**Part of Tree**	**A**	**B**	**r^2**
2015 (15D)	Stem	86.014	0.0667	0.93
	Branch	8.8055	0.078	0.85
	Leaf	4.549	0.0825	0.93
	Root		(aboveground biomass [1]) × 0.35 [a]	

* RT, rotation of coppices. Total biomass (oven-dried tonnes, Mg) was obtained based on these data according to [ODT = A × e^{BD}], where A and B are coefficients of the regression parameter to be determined, D is the DBH (mm) and ODT is the dry weight of aboveground (oven dry tons (Mg) ha^{-1} y^{-1}). [1] Aboveground biomass is sum of stem, branch and leaf biomass, [a] root biomass [37,38], the coefficient estimation method is based on biomass data collected in October 2013, 2014 and 2015, respectively.

To investigate the potential of carbon storages in SRCs, we analyzed the carbon content (%) of the biomass and multiplied it with the dry mass. Poplar tree samples were harvested in October 2015 and oven-dried at 70 °C for 96 h after being weighed for the fresh weight of poplar stems. Stems (upper parts and lower parts) were selected from three different sites (SRC2012, 2013 and 2014) for analysis. Samples were chipped and broken down using a crusher and air-dried at room temperature again. The material was then sorted into powder using 60–80 mesh (testing sieve grid area: 1 mm) and 40–60 mesh (testing sieve grid area: 425 μm). The carbon contents of poplar samples grown in SRC of reclaimed land were analyzed via an elemental analyzer (Flash EA 1112, Thermo, MA, USA) with thermal conductivity detector (TCD). The amount of CO_2 absorption was also calculated by using their molecular weight [38]. It is generally known that the carbon content (carbon fraction) of woody plants studied in previous studies is 50% of their dry mass [39–42]. However, biomass and carbon coefficient can be changed in many ways due to environmental and various conditions, even if there are same species [43]. Thus, we analyzed the carbon content of poplar grown in Saemangeum reclaimed land, and used this value (average 46%) as a coefficient for estimating the carbon storage of poplar trees. The formula we used is as follows: Carbon storage (gC) = Total biomass × 0.46 (carbon content of poplar, %), Carbon dioxide absorption volume (gCO_2) = carbon storage × 44 (molecular weight of carbon dioxide) × [12 (molecular weight of carbon)]$^{-1}$ (Equations (4) and (5)).

$$\text{Carbon storage } (gC) = T\ (g) \times 0.46 \quad (4)$$

$$\text{Carbon dioxide absorption volume } (gCO_2) = T\ (g) \times 0.46 \times 44/12 \quad (5)$$

where T is the dry weight of the aboveground biomass of polar trees.

2.3. Change of Neighboring Herbaceous Vegetation

To characterize the plant diversity and ground flora distribution around the studied SRC, we monitored changes in the actual vegetation and the structure of the herbaceous vegetation in plots (5 m × 5 m) in the area (from 5 to 9 plots per 0.1 ha in the SRC) planted with *Populus* × *Canadensis* Moench. and in neighboring vegetation of SRC, in October 2013, 2014 and 2015, respectively. Based on collected data, we classified the type of the plant occurred in SRC and its neighboring vegetation, and investigate dominant species in each site, frequency of occurred plant, their relative density, and number of plants per ha. All data were calculated by the method of Braun-Blanquet and Taylor [44,45]. The formula we used is as follows: (Equations (6)–(8)).

$$\mathrm{F}\ (\%) = \mathrm{N_{AS}} \times \mathrm{N_T} \times 10^2 \tag{6}$$

$$\mathrm{RD}\ (\%) = \mathrm{N_{SS}} \times \mathrm{N_{TS}} \times 10^2 \tag{7}$$

$$\mathrm{N}\ (\mathrm{EA\ ha^{-1}}) = (\mathrm{N_T} \times \mathrm{N_{PS}}) / (\mathrm{N_P} \times 25) \times 10^4 \tag{8}$$

where F is the frequency, N_{AS} is the number of plots appeared specific species, N_T is the number of total plot in filed site, RD is the relative density, N_{SS} is the number of specific plant species among all plot of specific site, N_{TS} is the number of total species appeared in all plot of specific site, N is the number of plants per ha, N_T is the number of specific plant species that appeared in all plots of a specific site, N_{PS} is the number of specific plant species that appeared in all plots of a specific site, N is the number of plots, N_T is the number of specific plant species that appeared in all plots of a specific site, and N_{PS} is the number of plots.

2.4. Energy Value and Pellet Criteria

Harvested poplar tree samples were chipped and broken down using a crusher and air-dried at room temperature. The material was then sorted into powder using 60–80 mesh (testing sieve grid area: 1 mm) and 40–60 mesh (testing sieve grid area: 425 μm). Its known toxic chemical substance emission is problematic because of increased contents of N, Cl, S, and heavy metals when fuel pellets burn. To evaluate their contents, this parameter (%) was chosen following the Korean criteria for wood pellet quality [46], Pellet Fuels Institute standard specifications of United States [47], and EN-Plus standard specifications of European Union [48]. Each of those standards defines three or four quality classes: 1st grade (G1 or Premium, A1), 2nd grade (G2 or Standard, A2), 3rd grade (G3 or Utility, B), and 4th grade (G4), based on the range values of specific parameters, with ash content or calorific value as the most important. The physical and chemical parameters (toxic substance emissions) that were taken into account in this study are shown in Appendix E. Specific analyzer assays on pellet criteria were calculated by the method and equipment employed by Jang et al. [31] with an isoperibol oxygen bomb calorimeter (Parr 6400, Parr, IL, USA), electric muffle furnace (J-FM3, JISICO, Seoul, Korea), inductively coupled plasma (Atomscan 25, Thermo Jarrell Ash, Franklin, TN, USA), ion chromatography (Sykam S-134) and an elemental analyzer (Flash EA 1112, Thermo, Waltham, USA) (Equations (9) and (10)).

$$Q_\mathrm{d}\ (\mathrm{MJ\ kg^{-1}}) = \mathrm{Q_{dm}} / \mathrm{m_{ds}} \tag{9}$$

where Q_d is the net calorific value per weight of measured dry mass, Q_{dm} is the calorific value of the measured dry mass, and m_{ds} is the dry weight of the measured sample.

$$\mathrm{Ash}\ (\%) = \mathrm{W}\ (\mathrm{g}) / \mathrm{D}\ (\mathrm{g}) \times 100 \tag{10}$$

where Ash is the ash content of dry mass, W is the weight after the oxidation of the sample, and D is the dry weight of the sample.

2.5. Volumetric Soil Moisture Content

Tree growth is heavily influenced by climatic conditions, and soil moisture may be particularly important to measure drought influence with precipitation records and soil chemical properties. Thus, soil moisture may be particularly important [49]. For this study, we define drought as soil moisture deficit caused by insufficient rainfall [50]. Soil water content reflectometers (CS616, Cambell Scientific, Logan, UT, USA) were installed at two locations to determine soil's volumetric moisture content. Sensors were inserted horizontally at 30 cm below the interface. The data recordings were taken at one-hour time steps, and the Campbell Scientific calibration equation was used to calculate the volumetric moisture content. The volumetric soil moisture content (VSM, %) was very similar for both locations, so only one location is presented in the results (Figure 1).

2.6. Soil Chemical Properties

Soil samples were collected from the area of the SRC during the experimental period (0–20 depth; surface soil; Ap layer). The sampled soil was oven-dried at 60 °C for 48 h, and the oven-dried soil samples were analyzed for their chemical and physical properties. The electrical conductivity (EC) and pH values were determined using EC and pH meters (S230 and MP230, respectively, from Mettler Toledo, Greifensee, Switzerland) at a soil-to-water ratio of 1:5 (*w*/*v*). Total nitrogen was determined by the Kjeldahl method with a Kjeltec 2300 Auto Analyzer (Foss, Hillerød, Denmark) [51] (Equations (11)). Organic matter was determined using the method described by Walkely and Black [52]. Available phosphorus was determined by the method of Bray and Kurtz [53].

$$\text{Total nitrogen } (\%) = (\text{T} - \text{B}) \times \text{f} \times \text{N} \times 14 \times 100\text{w}^{-1} \times 100\text{s}^{-1} \quad (11)$$

where T is the standard solution of sulfuric acid (mL), B is the standard solution of sulfuric acid for using blank titration (mL), f is the correction value of the standard solution of sulfuric acid, N is the normality of the standard solution of sulfuric acid, w is the weight of the sample (mg), and s is the amount of used filtrate (mL)

2.7. Quantification of Photosynthetic Pigments

To investigate foliar photosynthetic pigment measurements, poplar leaves were collected in June and October 2013, 2014 and 2015 to measure the contents of chlorophyll a and b and carotenoid. Chlorophyll (Chl) and carotenoid (Car) were extracted from 0.1 g leaf discs using 10 cm^3 of an 80% acetone solution in a brown vial for one week at 4 °C. Absorbance was measured using a spectrophotometer at wavelengths of 663, 645, and 470 nm with a microplate reader (Epoch, Bio-Tek, Winooski, VT, USA). Chlorophyll contents (chlorophyll a, chlorophyll b, and total chlorophyll) and total carotenoid were calculated using the method of Arnon [54] (Equations (12)–(15)).

$$\text{Chlorophyll a } (\text{mg g}^{-1}\,\text{FW}) = 12.7 \times \text{A} - 2.69 \times \text{B} \quad (12)$$

$$\text{Chlorophyll b } (\text{mg g}^{-1}\,\text{FW}) = 22.9 \times \text{B} - 4.68 \times \text{A} \quad (13)$$

$$\text{Total chlorophyll } (\text{a} + \text{b}) \ (\text{mg g}^{-1}\,\text{FW}) = 20.2 \times \text{B} - 8.02 \times \text{A} \quad (14)$$

$$\text{Total carotenoid } (\text{mg g}^{-1}\,\text{FW}) = (1000 \times \text{C} - 1.82 \times \text{Chl a} - 85.02 \times \text{Chl b})/198 \quad (15)$$

where FW is fresh weight, A, B and C are pigment concentration, calculated as mg g^{-1} of FW from a 1 g m^{-3} cuvette of extract, A is the absorbance of the extract solution in a 1 cm path-length cuvette at wavelength 663 nm, B is the absorbance at 645 nm, and C is the absorbance at 470 nm.

2.8. Measurement of Photosynthetic Gas Exchanges

To investigate foliar photosynthetic gas exchanges, sampled poplar leaves were collected in June and October 2013, 2014 and 2015 to measure the net photosynthetic rate, stomatal conductance, transpiration rate and water-use efficiency. The branches sampled in the field were re-cut underwater and provided with a water supply. After this initial preparation, these parameters were measured with a Li-6400XT portable photosynthesis system (Li-Cor Inc., Lincoln, NE, USA) fitted with a 6400-02B red/blue LED light source. The measurements were taken on the third to fifth fully expanded leaves from the top of each plant for each treatment. All gas exchange measurements were conducted with the CO_2 concentration set at 400 μmol·mol^{-1}, at an air temperature of 25 °C and a relative humidity of 50–60%. Photosynthetic photon flux density (PPFD, μmol·m^{-2}·s^{-1}) was adjusted to ambient levels determined outside the treatments immediately prior to initiation of the sampling procedure. Photosynthetic water use efficiency (WUE, the ratio of photosynthetic rate to transpiration rate) was calculated using the following method (Equation (16)).

$$\text{WUE } (\mu\text{mol mmol}^{-1}) = (\text{Pn } (\mu\text{mol m}^{-2}\text{s}^{-1})/(\text{Tr } (\text{mmol m}^{-2}\text{s}^{-1})) \quad (16)$$

where Pn is the photosynthetic rate (μmol m^{-2} s^{-1}) and Tr is the transpiration rate (mmol m^{-2} s^{-1}). Diurnal patterns of photosynthetic parameters were evaluated from 09:00 to 12:00 during the experimental period in June and October 2013, 2014 and 2015.

2.9. Statistical Analysis

We used a t-test and an analysis of variance (ANOVA) to determine whether biomass yield, photosynthetic parameters changes among three sites (SRC2012, 2013 and 2014) during the wet (13W, 14W) and dry (15D) years, and which seasons/rotations had a variation in net growth, photosynthetic pigment and gas exchange flux. All statistical analyses of experimental data between different environmental conditions were performed with SPSS Statistics version 23 for Windows (SPSS, Chicago, IL, USA). Least significant difference calculations among the mean values were performed by one-way ANOVA and Tukey's post-tests at a p value of 0.05 for post hoc comparisons. Data analysis in 2013 SRC was done by independence t-test to find statistical significances of differences between the two site conditions (wet and dry) ($p \leq 0.05$).

3. Results

3.1. Biomass, Carbon Storage, and CO_2 Absorption

Based on the coefficient of estimated equation for biomass yield, total biomass potential (above and belowground) is predicted to be 195.49 Mg (81.98 Mg 2.3 ha^{-1} 3 yrs^{-1} (SRC2012); 72.87 Mg 19 ha^{-1} 3 yrs^{-1} (SRC2013); 40.64 Mg 34.3 ha^{-1} 3 yrs^{-1} (SRC2014)) (Stem, 103. 07 Mg 55.6 ha^{-1} 3 yrs^{-1}; Branch, 18.14 Mg 55.6 ha^{-1} 3 yrs^{-1}; Leaf, 23.59 Mg 55.6 ha^{-1} 3 yrs^{-1}; Root 50.68 Mg 55.6 ha^{-1} 3 yrs^{-1}). Furthermore, the aboveground stem biomass, as a main raw material for wood pellet production, in this SRC was calculated to be 103.07 Mg 55.6 ha^{-1} 3 yrs^{-1} (46.42 Mg 2.3 ha^{-1} 3 yrs^{-1} (SRC2012); 36.5 Mg 19 ha^{-1} 3 yrs^{-1} (SRC2013); 20.15 Mg 34.3 ha^{-1} 3 yrs^{-1} (SRC2014)), and the carbon stock and CO_2 absorption volume (based on total biomass) were calculated to be 89.92 MgC 55.6 ha^{-1} 3 yrs^{-1} (37.71 Mg 2.3 ha^{-1} 3 yrs^{-1} (SRC2012); 33.52 Mg 19 ha^{-1} 3 yrs^{-1} (SRC2013); 18.69 Mg 34.3 ha^{-1} 3 yrs^{-1} (SRC2014)), 329.72 MgCO_2 55.6 ha^{-1} 3 yrs^{-1}(138.27 Mg 2.3 ha^{-1} 3 yrs^{-1} (SRC2012); 122.91 Mg 19 ha^{-1} 3 yrs^{-1} (SRC2013); 68.54 Mg 34.3 ha^{-1} 3 yrs^{-1} (SRC2014)), respectively (Tables 3 and 4). The biomass production and carbon stock are shown in Tables 3 and 4.

Table 3. Biomass yield and carbon storage of poplar grown in short rotation coppice in Saemangeum reclaimed land throughout 2013, 2014 and 2015.

Sites	AR (ha)	RT (Tree Age)	MH (m)	MD (cm)	Biomass (ODT (Mg) ha^{-1})					C (MgC ha^{-1})	CO_2 (MgCO_2 ha^{-1})
					Stem	Branch	Leaf	Root	Total		
2012 [a]	2.3	13W [X] (1)	2.8	1.5	3.5	0.8	0.9	1.8	7.02	3.2	11.8
		14W [Y] (2)	4.5	2.9	14.1	3.1	1.9	6.6	25.8	11.8	43.5
		15D [Z] (3)	6.3	4.2	20.2	3.8	2.5	9.2	35.6	16.4	60.1
2013 [b]	19	13W (NA)						–			
		14W (1)	1.8	1.5	1.3	0.5	0.3	0.73	1.5	0.7	2.5
		15D (2)	2.9	2.6	1.9	0.4	0.5	0.9	3.8	1.7	6.5
2014 [c]	34.3	13W (NA)						–			
		14W (NA)						–			
		15D (1)	1.3	1.9	0.6	0.05	0.2	0.3	1.2	0.5	2.0
Total	55.6		3.5	2.9	2.9	4.2	3.2	10.5	40.6	18.7	68.6

AR, area; RT, rotation of coppices; cultivated period (1–3 years; Arabic number) for RT is shown in brackets; MH [c], mean tree height; MD [d], mean diameter at breast height; C, carbon storage; CO_2, carbon absorption volume; ODT, oven-dried tonnes (Mg), carbon storage (g C) = total biomass × 0.46 (carbon content of poplar, %), carbon dioxide absorption volume (g CO_2) = carbon storage × 44 (molecular weight of carbon dioxide) × [12 (molecular weight of carbon)]–1, all samples were collected every October 2013, 2014 and 2015 except for root biomass. [X] 13W, collected data in first rotation with wet season in 2013; [Y] 14W, collected data in second rotation with wet season in 2014; [Z] 15D, collected data in third rotation with dry season in 2015. [a] 2012, plot of short-rotation coppice (SRC) established in 2012 (density, 1 m × 1 m). [b] 2013, plot of short-rotation coppice (SRC) established in 2013 (density, 1 m × 1 m). [c] 2014, plot of short-rotation coppice (SRC) established in 2014 (density, 1 m × 1 m). "–" means unsprouted and/or unafforested area. NA, no value has been established.

Table 4. Estimated value of biomass yield and carbon storage of poplar grown in short rotation coppice in Saemangeum reclaimed land based on study area.

Sites (ha)	Biomass (ODT (Mg) 2.3 ha^{-1})					C (MgC 2.3 ha^{-1})	CO_2 (MgCO_2 2.3 ha^{-1})
	Stem	Branch	Leaf	Root	Total		
2012 [a] (2.3)	46.42	8.68	5.68	21.25	81.98	37.71	138.27
Sites (ha)	**Biomass (ODT (Mg) 19 ha^{-1})**					**C (MgC 19 ha^{-1})**	**CO_2 (MgCO_2 19 ha^{-1})**
	Stem	**Branch**	**Leaf**	**Root**	**Total**		
2013 [b] (19)	36.50	7.75	9.73	18.89	72.87	33.52	122.91
Sites (ha)	**Biomass (ODT (Mg) 34.3 ha^{-1})**					**C (MgC 34.3 ha^{-1})**	**CO_2 (MgCO_2 34.3 ha^{-1})**
	Stem	**Branch**	**Leaf**	**Root**	**Total**		
2014 [c] (34.3)	20.15	1.76	8.19	10.54	40.64	18.69	68.54
Sites (ha)	**Biomass (ODT (Mg) 55.6 ha^{-1})**					**C (MgC 55.6 ha^{-1})**	**CO_2 (MgCO_2 55.6 ha^{-1})**
	Stem	**Branch**	**Leaf**	**Root**	**Total**		
Total (55.6)	103.07	18.14	23.59	50.68	195.49	89.92	329.72

C, carbon storage; CO_2, carbon absorption volume; ODT, oven-dried tonnes (Mg), carbon storage (g C) = total biomass × 0.46 (carbon content of poplar, %), carbon dioxide absorption volume (g CO_2) = carbon storage × 44 (molecular weight of carbon dioxide) × [12 (molecular weight of carbon)] − 1, all samples were collected every October 2013, 2014 and 2015 except for root biomass. [a] 2012, plot of short-rotation coppice (SRC) established in 2012 (density, 1 m × 1 m). [b] 2013, plot of short-rotation coppice (SRC) established in 2013 (density, 1 m × 1 m). [c] 2014, plot of short-rotation coppice (SRC) established in 2014 (density, 1 m × 1 m).

In SRC 2012, during the three-year study, the annual net height growth of poplar seedling was highest in 1.03 m y^{-1} on the second rotation (14W), followed by 0.79 m y^{-1} on the third rotation (15D) and 0.78 m y^{-1} on the first rotation (13W) ($p < 0.05$). However, the annual net growth of diameter was not significantly different among the three different rotations (Figure 2).

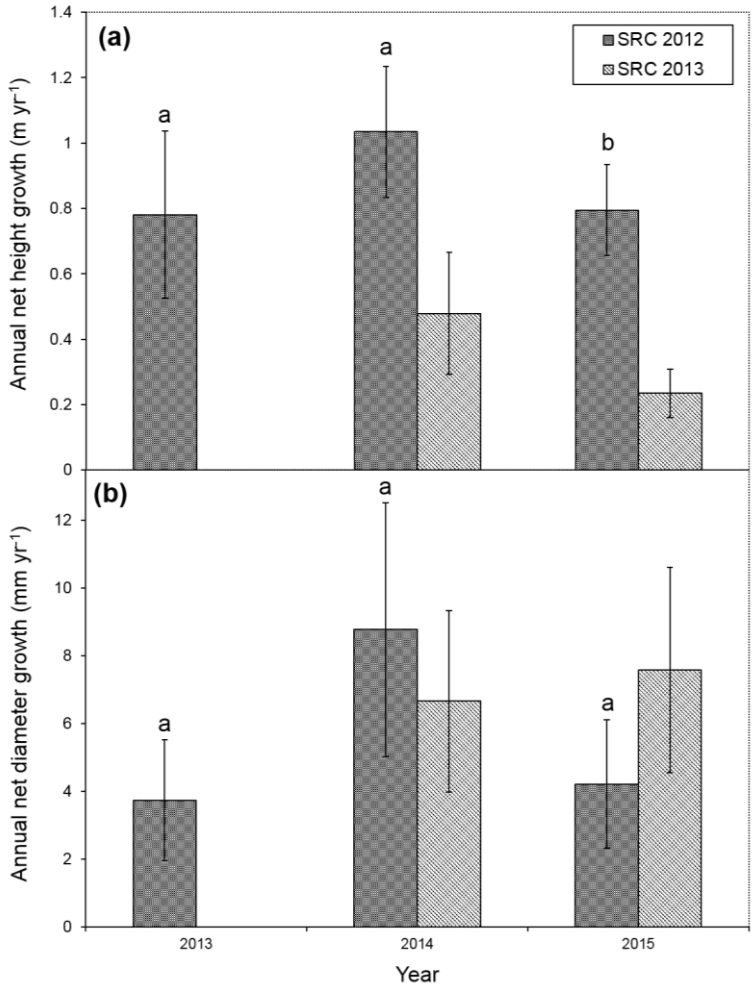

Figure 2. Annual net height growth (**a**); annual net diameter growth (**b**) for the study site (SRC 2012, 2013) throughout 2013, 2014 and 2015. Data were analyzed using one-way ANOVA and Tukey's post-test. Different letters in the same column represent significant differences at $p \leq 0.05$.

3.2. Fuel Pellet Utilization

To investigate whether whole wood material, such as wood pellets, is suitable for producing biofuel, we analyzed the net calorific value (Q), ash content, and amounts of toxic chemical substance, and heavy metal content of dry mass (Table 5). According to the results, biomass produced at this site yielded third grade pellets (G3), and its calorific value (Q) for generating heating energy was established to be equal to that of first grade (G1) pellets. All data obtained (Q, ash content, N, Cl, S, As, Cd, Cr, Cu, Pb, Hg, Ni and Zn) were very similar for three years (rotation), so only one dataset analyzed in 2015 is presented in the results.

3.3. Changes of Physical and Chemical Properties in Pedosphere

Soil samples of three different SRC afforestation sites (SRC 2012, 2013 and 2014) were collected during the experimental period in 2013, 2014 and 2015, respectively, and analyzed for pH, EC, organic matter, total nitrogen (T-N), available phosphorus (avail. P), sodium chloride content, texture, and exchangeable cations. The results are as follows (Table 6).

Table 5. Net calorific value, ash content, toxic chemical substance (N, Cl, S), heavy metal content of dry mass produced in short rotation coppice in Saemangeum reclaimed land.

Q (MJ kg^{-1})	Ash Content (%)	N (%)	Cl (%)	S (%)
18.8–19.4 * (0.39)	1.20–1.65 ** (0.20)	0.79–0.94 ** (0.50)	0.0012–0.006 * (0.00)	0.022–0.026 * (0.00)
>18.0 [z]	<3.0	<1.0	<0.05	<0.05

As	Cd	Cr	Cu	Pb	Hg	Ni	Zn
			(mg kg^{-1})				
N.D [a,*]	0.3–0.5 * (0.08)	0.4 * (0.00)	4–5 * (0.42)	0.2–0.4 * (0.08)	N.D [a,*]	N.D [a,*]	18–20 * (0.93)
≤1	≤0.5	≤10	≤10	≤10	≤0.05	≤10	≤100

* First grade (G1), ** third grade (G3), [z] the grade criteria of wood pellet, [a] not detectable (National Institute of Forest Science 2015) [46], *Q* net calorific value, All samples were collected in October 2015 except for root biomass. SD(s) for net calorific value, ash content, toxic chemical substance and heavy metal content of drymass is shown in brackets. All data obtained (*Q*, ash content, N, Cl, S, As, Cd, Cr, Cu, Pb, Hg, Ni and Zn) were very similar for three years (rotation), so only one dataset analyzed in 2015 is presented in the results.

Table 6. Soil condition (0–20 depth) of SRC established in Saemangeum reclaimed land throughout 2012, 2013 and 2014.

Sites	$pH_{(1:5)}$	$EC_{(1:5)}$ (dS m^{-1})	OM (%)	CEC (cmol kg^{-1})
2012	7.7	0.08	2.0 [a]	7.9 [a]
2013	7.4	0.10	1.16 [b]	7.89 [a]
2014	7.6	0.11	0.66 [c]	7.82 [a]

Sites	avail. P (mg kg^{-1})	T-N (%)	NaCl (%)	Texture
2012	16.5 [a]	0.16 [a]	0.005 [a]	SiL
2013	15.29 [ab]	0.06 [ab]	0.006 [a]	SiL
2014	13.19 [b]	0.04 [ab]	0.007 [a]	SiL

Sites	K	Na	Mg	Ca
		(cmol kg^{-1})		
2012	0.01	0.01	0.01	0.01
2013	0.01	0.01	0.01	0.01
2014	0.01	0.01	0.01	0.01

pH, potential of hydrogen. EC, electrical conductivity. OM, organic matter. avail. P, available phosphorus, T-N, total nitrogen, SiL, silt loam. All samples were collected in October 2013, 2014 and 2015, respectively, except for root biomass. One-way ANOVA test was performed to evaluate the differences among three sites (2012, 2013 and 2014). Post hoc comparisons were performed using the Tukey's post-test at a significance level of $p \leq 0.05$. Different alphabetical letters in the same column (OM, CEC avail. P, T-N and NaCl of three sites) represent significant differences according to independent samples at $p \leq 0.05$.

In general, reclaimed land in Korea has a high level of soluble salts and exchangeable sodium, which hinders the growth of the plants; however, this constraint may be reduced by the level of fertility [30]. The soil characteristics of the SRC in the Saemangeum land reclamation project area appear to be similar with those of the forest soil in terms of low salinity [13]. However, soil nutrients, total nitrogen (T–N), and available phosphorus (avail. P) were lower in the SRC soil than in the forest soil. In our results, organic matter, avail. P and T–N were the highest in SRC 2012, followed by 2013 and 2014 ($p \leq 0.05$), whereas the sodium chloride and CEC were more increased in SRC 2014 than others, but this was not significantly different. Based on this soil condition, we monitored annual patterns and pedosphere type by dividing moderate (13W, 14W) and low fertility (15D). The soil volumetric moisture content at 30 cm and soil temperature at 30 cm below the surface were investigated in three different SRC afforestation sites (SRC 2012, 2013 and 2014). At this site, these values are recorded approximately 28.5% (maximum: 34% minimum 21%) and 15.3 °C (maximum: 30.1 °C, minimum 0.7 °C), respectively, and the moisture content during the peak growing season (June–August) in 2013 (13W), 2014 (14W) and 2015 (15D) was 27.63, 30.26 and 27.17%, respectively (Figure 1). Based on recorded precipitation and soil moisture conditions, we can confirm that a low rainfall event was

recorded in May–Jun in 2015 compared with last two years (2013–2014), and this period also showed low soil moisture contents (%) in May–Jun 2015 (25.30 ± 2.1) compared with that of 2013 (28.50 ± 2.3) and 2014 (32.20 ± 1.2) ($p \leq 0.05$). Therefore, we monitored seasonal and annual pattern by dividing wet or moderate conditions (2013, 2014) and drought (2015).

3.4. Changes in the Flora Distribution of SRC and Neighboring Vegetation

The changes in flora distribution on the SRC in the Saemangeum area were monitored for 3 years. Our results show the changes in dominant species and species composition in the SRC 2012, 2013, and 2014, and the neighboring vegetation of SRC2012, 2013 and 2014, respectively (Tables 7–9). In site 2012, the dominant species during the period of first rotation (13W) and second rotation (14W) were *Aster subulatus* Michx. (halophyte) (46.67%) and *Setaria viridis* (halophyte) (26.67%), respectively. Moreover, the dominant species during the third rotation (15D) was also *S. viridis* (halophyte) (28.57%). The neighboring vegetation of site 2012 (NV2012) were dominant in *Phragmites communis* Trin (halophyte) (66.67%) for three years (first, second and third rotation), showing 100% frequency from the second rotation (14W) to the third rotation (15D). Even if glycophyte appeared on the first rotation, the dominant species was occupied by halophyte for three years. In SRC 2013, the dominant species was only *Echinochloa crus-galli* (L.) P.Beauv. (halophyte) (100%) on the first rotation (14W) and second rotation (15D), showing a contrasting pattern (glycophyte, 66.67%), even if a new halophyte species appeared (33.34%) during the second rotation. The neighboring vegetation of site 2013 (NV2013) was dominated by both *P. communis* Trin. (halophyte) and *Echinochloa crus-galli* var. *echinatum* (Willd.) Honda (glycophyte), equivalently, in the first year (14W). However, the vegetation of the second year (15D) is slightly dominated by *Calamagrostis epigeios* (halophyte). In SRC 2014, the most recently afforested site (15D), *Echinochloa crus-galli* (L.) P.Beauv. (halophyte) appeared as a dominant species (77.78%), followed by *S. viridis* (halophyte, 22.22%). On the contrary, the neighboring vegetation of site 2014 had two glycophyte species (*Aster subulatus* var. *sandwicensis* and *Echinochloa crus-galli* var. *echinatum* (Willd.) Honda) and one halophyte species (*Calamagrostis epigeios*), but the dominant species was glycophyte. Overall, among all investigated ground vegetation species, halophytes were recorded as a dominant vegetation species in SRC2012 and NV2012 during the 14W and 15D. However, the frequency of glycophyte (66.67%) increased in the second rotation (15D) compared with that of the first rotation (14W) in SRC2013. In terms of plant diversity, our studied SRC site showed a mean numbers of species (MN) ranging from 5.2 to 6.2 (SRC2012), and from 4.0 to 5.3 (NV2012), respectively. Meanwhile, in, SRC2013 and NV2013, this number was 3.3–5.3 and 4.5–5.0, respectively. In the case of herbaceous vegetation in SRC 2014 and NV2014, NV2014 has a higher species number (7.0) than SRC2014 (5.1) (see Tables 7–9).

Table 7. Change in herbaceous vegetation of SRC established in 2012 in Saemangeum reclaimed land over time.

Sites	RT (Tree Age)	Species	CL	MN	DS	F (%)	RD (%)	*n* (EA ha^{-1})
SRC2012	13W ^{X} (1)	*Setaria viridis*	H	6.2 (0.42)		33.33	36.56	2000
		Phragmites communis Trin.	H			13.33	16.13	800
		Echinochloa crus-galli (L.) P.Beauv.	H			6.67	8.60	400
		Aster subulatus Michx.	H		+	46.67	38.71	2800
	14W ^{Y} (2)	*Sonchus brachyotus*	H	6.0 (1.20)		20.00	16.67	1200
		Setaria viridis	H		+	26.67	23.33	1600
		Phragmites communis Trin.	H			20.00	22.22	1200
		Panicum bisulcatum	G			13.33	15.56	800
		Calamagrostis epigeios	H			13.33	14.44	800
		Setaria faberi	H			6.67	7.78	400
	15D ^{Z} (3)	*Setaria viridis*	H	5.2 (1.12)	+	28.57	31.51	1600
		Phragmites communis Trin.	H			21.43	17.81	1200
		Panicum bisulcatum	G			7.14	6.85	400
		Calamagrostis epigeios	H			21.43	19.18	1200
		Aster subulatus var. *sandwicensis*	G			21.43	24.66	1200

Table 7. *Cont.*

Sites	RT (Tree Age)	Species	CL	MN	DS	F (%)	RD (%)	*n* (EA ha^{-1})
NV2012	13W ^{X} (1)	*Aster subulatus* Michx.	H	5.3 (1.21)		33.33	37.50	800
		Phragmites communis Trin.	H		+	66.67	62.50	1600
	14W ^{Y} (2)	*Phragmites communis* Trin.	H	5.2 (0.98)	+	100.00	100.00	2400
	15D ^{Z} (3)	*Phragmites communis* Trin.	H	4.0 (0.0)	+	100.00	100.00	1200

RT, rotation of coppices; cultivated period (1–3 years; Arabic number) for RT is shown in brackets; MN, mean number of species; SD for MN is shown in brackets. CL, classification; H, halophyte (salt tolerant); G, glycophyte (salt sensitive). F (%) = [number of plots appeared specific species] × [number of total plot (5 m × 5 m) in field site]$^{-1}$ × 10^2. RD (%) = (number of specific plant species among all plot of specific site) × (number of total species appeared in all plot of specific site)$^{-1}$ × 10^2. *n* (EA ha^{-1}) = [the number of specific plant species appeared in all plot of specific site] × [(the number of specific plant species appeared in all plot of specific site) × (the number of plots × plot area (5 m × 5 m))$^{-1}$]$^{-1}$ × 10^4. DS, dominant species, F, frequency, RD, relative density, *n* = number of plants per ha. Sites: SRC2012, plot of short-rotation coppice established in 2012 (2-year-old seedlings grown for 3 years; density, 1 m × 1 m); NV2012, plot of neighboring vegetation (NV) surrounding SRC established in 2012. "+" means dominant plant species in this site. ^{X} 13W, collected data in first rotation with wet season in 2013; ^{Y} 14W, collected data in second rotation with wet season in 2014; ^{Z} 15D, collected data in third rotation with dry season in 2015.

Table 8. Change in herbaceous vegetation of SRC established in 2013 in Saemangeum reclaimed land over time.

Sites	RT (Tree Age)	Species	CL	MN	DS	F (%)	RD (%)	*n* (EA ha^{-1})
SRC2013	13W ^{X} (NA)			NA				
	14W ^{Y} (1)	*Echinochloa crus-galli* (L.) P.Beauv.	H	3.3 (1.03)	+	100.00	100.00	2400
	15D ^{Z} (2)	*Aster subulatus* var. *sandwicensis*	G	5.3 (0.82)	+	66.67	68.75	1600
		Setaria viridis	H			16.67	12.50	400
		Phragmites communis Trin.	H			16.67	18.75	400
NV2013	13W ^{X} (NA)			NA				
	14W ^{Y} (1)	*Phragmites communis* Trin.	H	5.0 (1.41)	+	33.33	37.50	400
		Echinochloa crus-galli var. *echinatum* (Willd.) Honda	G		+	33.33	37.50	400
		Calamagrostis epigeios	H			33.33	25.00	400
	15D ^{Z} (2)	*Aster subulatus* var. *sandwicensis*	G	4.5 (1.87)		33.33	33.33	400
		Echinochloa crus-galli var. *echinatum* (Willd.) Honda	G			33.33	27.78	400
		Calamagrostis epigeios	H		+	33.33	38.89	400

RT, rotation of coppices; cultivated period (1–3 years; Arabic number) for RT is shown in brackets; MN, mean number of species; SD(s) for MN is shown in brackets. CL, classification; H, halophyte (salt tolerant); G, glycophyte (salt sensitive). F (%) = [number of plots appeared specific species] × [number of total plot (5 m × 5 m) in field site]$^{-1}$ × 10^2. RD (%) = (number of specific plant species among all plot of specific site) × (number of total species appeared in all plot of specific site)$^{-1}$ × 10^2. *n* (EA ha^{-1}) = [the number of specific plant species appeared in all plot of specific site] × [(the number of specific plant species appeared in all plot of specific site) × (the number of plots × plot area (5 m × 5 m))$^{-1}$]$^{-1}$ × 10^4. DS, dominant species, F, frequency, RD, relative density, *n* = number of plants per ha. Sites: SRC2013, plot of short-rotation coppice established in 2013 (2-year-old seedlings grown for 2 years; density, 1 m × 1 m); NV2013, plot of neighboring vegetation (NV) of SRC established in 2013. NA, no value has been established. "+" means dominant plant species in this site. ^{X} 13W, collected data in first rotation with wet season in 2013; ^{Y} 14W, collected data in second rotation with wet season in 2014; ^{Z} 15D, collected data in third rotation with dry season in 2015.

Table 9. Herbaceous vegetation of SRC established in 2014 in Saemangeum reclaimed land over time.

Sites	RT (Tree Age)	Species	CL	MN	DS	F (%)	RD (%)	*n* (EA ha^{-1})
SRC2014	13W [X] (NA)			NA				
	14W [Y] (NA)			NA				
	15D [Z] (1)	*Echinochloa crus-galli* (L.) P.Beauv.	H	5.1 (0.93)	+	77.78	78.26	2800
		Setaria viridis	H			22.22	21.74	800
NV2014	13W [X] (NA)			NA				
	14W [Y] (NA)			NA				
	15D [Z] (1)	*Aster subulatus* var. *sandwicensis*	G	7.0 (2.0)		33.33	23.81	40
		Calamagrostis epigeios	H			33.33	33.33	40
		Echinochloa crus-galli var. *echinatum* (Willd.) Honda	G		+	33.33	42.86	40

RT, rotation of coppices; cultivated period (1–3 years; Arabic number) for RT is shown in brackets; MN, mean number of species; SD(s) for MN is shown in brackets. CL, classification; H, halophyte (salt tolerant); G, glycophyte (salt sensitive). F (%) = [number of plots appeared specific species] × [number of total plot (5 m × 5 m) in field site]$^{-1}$ × 10^2. RD (%) = (number of specific plant species among all plot of specific site) × (number of total species appeared in all plot of specific site)$^{-1}$ × 10^2. *n* = [the number of specific plant species appeared in all plot of specific site] × [(the number of specific plant species appeared in all plot of specific site) × (the number of plots × plot area (5 m × 5 m))$^{-1}$]$^{-1}$ × 10^4. DS, dominant species, F, frequency, RD, relative density, *n* (EA ha^{-1}) = number of plants per ha. Sites: SRC2014, plot of short-rotation coppice established in 2014 (2-year-old seedlings grown for 1 year; density, 1 m × 1 m); NV2014, plot of neighboring vegetation (NV) of SRC established in 2014. NA, no value has been established. "+" means dominant plant species in this site. [X] 13W, collected data in first rotation with wet season in 2013; [Y] 14W, collected data in second rotation with wet season in 2014; [Z] 15D, collected data in third rotation with dry season in 2015.

3.5. Changes of Photosynthetic Pigment Contents

The changes in chlorophyll and carotenoid contents in the SRC in Saemangeum area were monitored for 3 years. Total chlorophyll concentrations of poplar trees in SRC 2012 were highest in the first rotation (13W), followed by the third rotation (15D) and the second (14W). The average value of the total chlorophyll in SRC 2013 plot in June and October in first rotation (14W) was 0.99 ± 0.48 mg g^{-1} of fresh weight (FW) and 0.91 ± 0.08 mg g^{-1} of FW, respectively. Meanwhile, the total chlorophyll content in the second rotation (15D) was 0.75 ± 0.19 mg g^{-1} of FW and 0.57 ± 0.17 mg g^{-1} of FW, respectively. The chlorophyll a/b ratio of poplar in SRC 2012 in June and October was increased in the second rotation (14W) (0.34 ± 0.02; 0.34 ± 0.02) compared with the first rotation (13W) (0.01 ± 0.00; 0.01 ± 0.00); however, this value was decreased in the third rotation (15D) (0.01 ± 0.00; 0.29 ± 0.01). The carotenoid content in the SRC 2012 in June and October had a similar pattern with total chlorophyll and a/b ratio (Table 10).

In 2013 SRC, the total chlorophyll, carotenoid content and a/b ratio were higher in the second rotation (15D) than in the first rotation (14W). However, the chlorophyll content (0.99 ± 0.48; 0.91 ± 0.08) was lower than the measured value in 13W, 14W and 15D in SRC 2012.

Table 10. Total chlorophyll and carotenoid contents and chlorophyll a/b ratio of poplar leaf grown in the short-rotation coppice in Saemangeum reclaimed land throughout 2012, 2013 and 2014.

Sites	RT	Chl a (mg g^{-1} FW)		Chl b (mg g^{-1} FW)		Chl_T (mg g^{-1} FW)		Chl a/b		Car (mg g^{-1} FW)	
		June	October	June	October	June	October	June	October	June	October
2012 +	13W X (1)	1.22 ± 0.06 Z	1.22 ± 0.06	0.26 ± 0.14	0.23 ± 0.02	1.58 ± 0.08 a**	1.54 ± 0.12 a***	0.01 ± 0.00 b**	0.01 ± 0.00 c**	0.44 ± 0.02 a**	0.43 ± 0.03 a**
	14W Y (2)	0.01 ± 0.00	0.01 ± 0.01	0.36 ± 0.02	0.36 ± 0.02	1.22 ± 0.48 a	1.02 ± 0.43 b	0.34 ± 0.02 a	0.34 ± 0.02 a	0.14 ± 0.03 b	0.16 ± 0.05 b
	15D Z (3)	0.02 ± 0.00	0.51 ± 0.14	0.33 ± 0.13	0.18 ± 0.05	1.24 ± 0.39 aA	0.70 ± 0.19 bA	0.01 ± 0.00 bA	0.29 ± 0.01 bA	0.13 ± 0.02 bB	0.13 ± 0.01 bA
2013 ++	13W (NA)					–					
	14W (1)	0.01 ± 0.00	0.02 ± 0.00	0.33 ± 0.13	0.28 ± 0.12	0.99 ± 0.48 a*	0.91 ± 0.08 a**	0.00 ± 0.00 a*	0.01 ± 0.00 b*	0.17 ± 0.06 a*	0.19 ± 0.01 a*
	15D (2)	0.01 ± 0.00	0.62 ± 0.30	0.19 ± 0.04	0.15 ± 0.05	0.75 ± 0.19 aA	0.57 ± 0.17 bA	0.01 ± 0.00 aA	0.29 ± 0.02 aA	0.13 ± 0.03 bB	0.14 ± 0.04 bA
2014 +++	13W (NA)					–					
	14W (NA)					–					
	15D (1)	0.02 ± 0.00	0.43 ± 0.10	0.21 ± 0.03	0.14 ± 0.04	0.85 ± 0.12 A*	0.57 ± 0.14 A*	0.01 ± 0.00 A*	0.30 ± 0.02 A*	0.20 ± 0.01 A*	0.16 ± 0.03 A*

RT, rotation of coppices. Cultivated period (1–3 years; Arabic number) for RT is shown in brackets. Chl a, chlorophyll a content of poplar leaves. Chl b, chlorophyll b content of poplar leaves. Chl_T, total chlorophyll content of poplar leaves. Chl a/b, chlorophyll a/b ratio of poplar leaves. Car, carotenoid content of poplar leaves. Z Mean ± SE (n = 15). "–" means unsprouted and/or unafforested area; NA, no value has been established; X 13W, collected data in first rotation with wet season in 2013; Y 14W, collected data in second rotation with wet season in 2014; Z 15D, collected data in third rotation with dry season in 2015. + 2012, plot of short-rotation coppice (SRC) established in 2012. ++ 2013, plot of short-rotation coppice (SRC) established in 2013. +++ 2014, plot of short-rotation coppice (SRC) established in 2014. One-way ANOVA test was performed to evaluate the differences among three sites (2012, 2013 and 2014). Post hoc comparisons were performed using the Tukey's post-test at a significance level of $p \leq 0.05$. Data analysis in 2013 SRC was done by independence t-test ($p \leq 0.05$). Different uppercase letters in the same column (three sites) represent significant differences among three SRC sites (pedospheric condition) of the same meteorological condition at $p \leq 0.05$, Different lowercase letters in the same column represent significant differences among different meteorological conditions (wet and drought of same site) of the same site, Asterisk in the same column represent significant differences among different meteorological conditions and pedospheric condition of the same poplar stand ages (1-year, first rotation), as determined by Tukey's post-test. Total chlorophyll, chlorophyll a/b ratio and carotenoid content with less than two different rotation or climate factor were excluded from the statistical analysis.

3.6. Changes of Photosynthetic Gas Exchange

The changes in leaf gas exchanges on the SRC in Saemangeum area were also monitored for 3 years. The net photosynthesis assimilation rate of poplar grown on the SRC in Saemangeum area was investigated in June and October 2013, 2014 and 2015, respectively.

During this period, the highest photosynthetic rate of poplar trees in SRC 2012 was highest in the second rotation (14W), followed by the second (13W) rotation and the third (15D) in both seasons (June and October). The average value of photosynthetic rate in SRC 2013 plot in June and October during the period of the first rotation (14W) showed a higher rate than that of the second rotation (15D), being measured as 23.77 ± 1.02 and 24.67 ± 1.65 μmol m^{-2} s^{-1}, respectively. Meanwhile, the photosynthetic rate of 15D (second rotation) in SRC 2013 was 19.96 ± 1.24 and 20.37 ± 0.83 μmol m^{-2} s^{-1}, respectively. In the same context of photosynthetic pigments, the transpiration rate of poplar in the SRC 2012 in June was increased in the second rotation (14W) (10.29 ± 0.22 mmol m^{-2} s^{-1}) compared with the first rotation (13W) (9.55 ± 0.21 mmol m^{-2} s^{-1}), whereas this value was significantly decreased in the third rotation (15D) (9.14 ± 0.01 mmol m^{-2} s^{-1}) ($p \leq 0.05$). The stomatal conductance of poplar in the SRC 2012 had a similar pattern to that of carbon assimilation (Table 11).

Table 11. Net photosynthetic rate and stomatal conductance, transpiration rate and water-use efficiency of poplar leaf grown in the short-rotation coppice in Saemangeum reclaimed land throughout 2012, 2013 and 2014.

Sites	RT	P_n (μmol m^{-2} s^{-1})		Gs (mol m^{-2} s^{-1})		Tr (mmol m^{-2} s^{-1})		WUE (mmol μmol^{-1})	
		June	October	June	October	June	October	June	October
2012 [+]	13W [X] (1)	22.72 ± 2.64 [Za]	22.89 ± 0.86 [b]	1.03 ± 0.06 [b***]	0.99 ± 0.00 [a***]	9.55 ± 0.21 [a**]	9.44 ± 0.00 [a***]	2.38 ± 0.25 [a]	2.42 ± 0.09 [b*]
	14W [Y] (2)	23.41 ± 1.31 [a]	27.07 ± 0.83 [a]	1.28 ± 0.08 [a]	0.92 ± 0.01 [b]	10.29 ± 0.22 [b]	8.87 ± 0.02 [b]	2.27 ± 0.12 [a]	3.05 ± 0.10 [a]
	15D [Z] (3)	17.66 ± 0.81 [bC]	19.41 ± 2.09 [cB]	0.90 ± 0.00 [cB]	0.92 ± 0.06 [bA]	9.14 ± 0.01 [cB]	8.85 ± 0.23 [bA]	1.93 ± 0.09 [bB]	2.20 ± 0.24 [cB]
2013 [++]	13W (NA)					–			
	14W (1)	23.77 ± 1.02 [a]	24.67 ± 1.65 [a]	0.99 ± 0.06 [a**]	0.73 ± 0.00 [b*]	9.56 ± 0.24 [a**]	8.29 ± 0.02 [b*]	2.49 ± 0.08 [a]	2.98 ± 0.20 [a**]
	15D (2)	19.96 ± 1.24 [bB]	20.37 ± 0.83 [bAB]	0.67 ± 0.00 [bC]	0.86 ± 0.00 [aB]	8.05 ± 0.01 [bC]	8.92 ± 0.02 [aA]	2.48 ± 0.15 [aA]	2.28 ± 0.09 [bB]
2014 [+++]	13W (NA)					–			
	14W (NA)					–			
	15D (1)	21.83 ± 2.09 [A]	22.46 ± 2.87 [A]	0.94 ± 0.01 [A*]	0.75 ± 0.00 [C**]	9.29 ± 0.04 [A*]	8.39 ± 0.01 [B**]	2.35 ± 0.22 [A]	2.68 ± 0.34 [A*]

RT, rotation of coppices. Cultivated period (1–3 years; Arabic number) for RT is shown in brackets. P_n, net photosynthetic rate of poplar leaves. Gs, stomatal conductance of poplar leaves. Tr, transpiration rate of poplar leaves. WUE, water-use efficiency of poplar leaves. [Z] Mean ± SE (n = 15). "–" means unsprouted and/or non-forested area; NA, no value has been established; [X] 13W, collected data in first rotation with wet season in 2013; [Y] 14W, collected data in second rotation with wet season in 2014; [Z] 15D, collected data in third rotation with dry season in 2015. [+] 2012, plot of short-rotation coppice (SRC) established in 2012. [++] 2013, plot of short-rotation coppice (SRC) established in 2013. [+++] 2014, plot of short-rotation coppice (SRC) established in 2014. One-way ANOVA test was performed to evaluate the differences among three sites (2012, 2013 and 2014). Post hoc comparisons were performed using the Tukey's post-test at a significance level of $p \leq 0.05$. Data analysis in 2013 SRC was done by independence t-test ($p \leq 0.05$). Different uppercase letters in the same column (three sites) represent significant differences among three SRC sites (pedospheric condition) of the same meteorological condition at $p \leq 0.05$, Different lowercase letters in the same column represent significant differences among different meteorological conditions (wet and drought of same site) of the same site, Asterisk in the same column represent significant differences among different meteorological conditions and pedospheric condition of the same poplar stand ages (1-year, first rotation), as determined by Tukey's post-test. Net photosynthetic rate, stomatal conductance, transpiration and water-use efficiency with less than two different rotation or climate factor were excluded from the statistical analysis.

In 2013 SRC, the photosynthetic carbon flux, stomatal conductance and transpiration rate also significantly decreased in the second rotation (15D) compared to the first rotation (14W) during the growing season (Jun) ($p \leq 0.05$). However, amongst the three different site conditions (SRC 2012, 2013 and 2014) and meteorological conditions (13W, 14W and 15D), the transpiration rate of poplar seedlings (same poplar stand ages; first rotation) was lowest in 15D in SRC 2014 (9.29 ± 0.04 mmol m^{-2} s^{-1}), compared with 14W in SRC2013 (9.56 ± 0.24 mmol m^{-2} s^{-1}) and 13W in SRC2012 (9.55 ± 0.21 mmol m^{-2} s^{-1}), respectively ($p \leq 0.05$).

4. Discussion

4.1. Biomass and Bioenergy Potential on Reclaimed Land

SRC cultures are gaining greater importance in stabilizing global climate change, such as drought, by mitigating increased atmospheric CO_2 proportionally as well as for the production of carbon neutral renewable bioenergy. We found that Korean biomass plantations via poplar trees have the potential to become a significant carbon-neutral source of renewable energy. Wood is regarded as an ideal composite that can be regenerated perpetually and is an important source material for industries [55]. Analysis of the organization of ingredients in wood is necessary to ensure that the wood can be efficiently used as an alternative for finite resources [56,57]. It is little known that unlike the development of paddy fields on reclaimed land, afforestation of reclaimed land has been conducted, despite the fact that, in general, plant species cannot survive on reclaimed land when the soil is still barren. Yeo et al. [58] reported that in SRC plantations on Korean reclaimed land, plant growth and biomass yield are more affected by

nutrient deficiency and imbalance and salinity level. Shin et al. [34] reported that on Korean reclaimed land, the biomass production of *Populus* × *Canadensis* Moench. clones is the highest among woody crop species. Moreover, Klasnja et al. [59] reported that the calorific values based on dry mass of *Populus* × *Canadensis* Moench. are different from those of *P. deltoides* and *Salix alba*. Their results show that *Populus* wood has the highest heating value for dry mass (calculated for the whole tree based on the proportion of bark). This study found that the biomass production of *Populus* × *Canadensis* Moench. in the SRC (total area, 55.6 ha) in the Saemangeum area was 195.49 Mg (81.98 Mg 2.3 ha^{-1} 3 yrs^{-1} (SRC2012); 72.87 Mg 19 ha^{-1} 3 yrs^{-1} (SRC2013); 40.64 Mg 34.3 ha^{-1} 3 yrs^{-1} (SRC2014)) (Stem, 103. 07 Mg 55.6 ha^{-1} 3 yrs^{-1}; Branch, 18.14 Mg 55.6 ha^{-1} 3 yrs^{-1}; Leaf, 23.59 Mg 55.6 ha^{-1} 3 yrs^{-1}; Root 50.68 Mg 55.6 ha^{-1} 3 yrs^{-1}); in addition, carbon storage and CO_2 absorption were calculated to be 89.92 Mg C (37.71 Mg 2.3 ha^{-1} 3 yrs^{-1} (SRC2012); 33.52 Mg 19 ha^{-1} 3 yrs^{-1} (SRC2013); 18.69 Mg 34.3 ha^{-1} 3 yrs^{-1} (SRC2014)) and 329.72 Mg CO_2 (138.27 Mg 2.3 ha^{-1} 3 yrs^{-1} (SRC2012); 122.91 Mg 19 ha^{-1} 3 yrs^{-1} (SRC2013); 68.54 Mg 34.3 ha^{-1} 3 yrs^{-1} (SRC2014)), respectively. In the case of Korea, biomass yield in SRC has different tendencies by poplar clone and site condition. Amongst poplar species, *Populus* × *Canadensis* Moench. was reported to have 17.6 Mg ha^{-1} y^{-1}, 31.2–33.5 Mg ha^{-1} 4 y^{-1} and 28.2–40.8 Mg ha^{-1} 5 y^{-1} on SRC established in an idle farmland or riparian area, respectively [60,61]. Manzone and Calvo [62] reported ideal rotation for sustainable biomass yield in SRC is with a 3 or 6 year rotation. Based on this rotation, 14 Mg ha^{-1} y^{-1} can be produced, and carbon accumulation by aboveground of SRC ranged from 3.89 to 6.48 MgC ha^{-1} y^{-1} [62,63]. Our results suggest that biomass yield in 1–2 years was lower than other types of SRC, but the production in 3 years showed a proper portion of yield compared with other sites based on our expectations. In general, 50% of the carbon content of deciduous trees is reported to be contained in the main body (stem) [39–41], but we investigated the content in more detail. Consequently, we noted that the carbon content of poplar in the SRC is different from that at other sites, but not lower than at forest sites (43%). Kim et al. [64] also reported that the carbon content of 2-year-old poplar in a short rotation coppice-grown riparian area was 47.1%. Thus, it is required to quantize the carbon coefficient in various land-use patterns, such as barren areas for sustainable SRC management [65]. Based on our estimation of carbon sequestration, it is expected to perform a key role in Saemangeuem SRC for not only wood energy output but also carbon sink or shelterbelt near the Yellow Sea of South Korea. Son et al. [66] reported that the carbon emission quantity in the automotive sector is 2.4 $MgCO_2$ ha^{-1} y^{-1} motor $vehicle^{-1}$ in South Korea, because our three sites (2012, 2013 and 2014) are estimated to absorb 2.0–11.8 $MgCO_2$ ha^{-1} y^{-1} during the first year of rotation (Table 3). In our study, it was revealed that poplar planted on Saemangeum area can remove the annual carbon emissions by motor vehicles efficiently. Many previous studies reported that a lack of precipitation, abundant PPFD and high summer temperature affect the decrease in biomass yield and produce a physiological effect in woody plants [67]. It was also reported that drought causes foliar acclimation via Gs, which is in turn associated with a reduction in C*i* along with light-saturated photosynthetic rates in C3 plants, such as poplar, due to mesophyll conductance (gm) limitations [68]. However increasing drought imposition can cause biomass yield loss with physiological changes, such as down-regulation of antioxidant systems [69] and root system allocation [63].

Amid dry conditions, in terms of sustainable SRC management, irrigation treatment might be necessary due to the severe summer drought [63], and CO_2 application could be required based on a previous study that showed that it mitigates drought stresses, enhancing photosynthetic potential in woody crops in SRCs [69]. Our team also confirmed that our site condition might also be vulnerable to sustainable biomass management on environmental factors such as drought and land-use changes (soil condition) if severe drought lasts over time. For these reasons, many previous studies have suggested and conducted nitrogen fertilization on SRCs [70]. Even if the fertilization rate positively affects fostering biomass yield, these benefits did not counterbalance environmental and economic aspects, because it might trigger another negative impact, such as nitrate leaching and N_2O emission [71]. Currently, environmental and economic analyses of the performance of the biomass supply chain for sustainable SRC management lie in the methodology of biomass collection after harvesting.

San Miguel et al. [72] reported that chip harvesting is more cost effective than bale harvesting, whereas transportation costs were decisive in the economic value of SRC. For sustainable SRC management, rental cost for land-use and less irrigation and fertilization management would play a crucial role to improve biomass yield.

The energy value grown in SRC on Saemangeum reclaimed land had a proper criteria despite the pedospheric condition being more barren (decreased soil organic matter) and the soil moisture content being changed due to a temporary drought condition with decreased precipitation. Generally, *Quercus mongolica*, a common wood species distributed in mountain forests of South Korea, has 19 MJ kg^{-1}–20 MJ kg^{-1} based on forest wood resources [73]. Compared with mountain forest resources, our result (18.8 MJ kg^{-1}–19.4 MJ kg^{-1}) was very efficient in producing bioenergy based on SRC management on a barren area and reserved land in a huge reclamation. In addition, SRC management is very efficient for carbon storage in soil, because the aboveground biomass:below ground biomass ratio is increased with aboveground biomass of a well-grown stand. This means that belowground biomass can be decreased by 14–21% compared with aboveground [73–75]. In other words, it is possible to maintain soil carbon sequestration with SRC management more easily than in forest ecosystems. However, it will be necessary to investigate the effect of short rotation of the forest on soil carbon sequestration, and belowground biomass of fast-growing trees. Once the dry mass, as a raw material for producing fuel pellets, is combusted, its mineral ash remains in oxidized form. Ash content and its chemical composition affect the smooth operation of gasifiers. During the gasification process, the ash contents fuse and their cohesion forms a mineral residue. No mineral debris is left if the ash content in the biomass is less than 5% [76]. An ash content of 0.7% is considered first grade, of 1.5% is considered second grade, and of less than 3.0% is considered third grade [46]. Compared with the Pellet Fuel Institute standard in the USA and the EU's EN-Plus standard, the specifications in the Korean wood pellet standard eliminate the disadvantages in the assessment criteria of both (Table 9). In this study, the quality of poplar for wood pellet production was evaluated to be first to third grade, indicating that wood pellets can be manufactured and produced profitably from poplar grown in the Saemangeum SRC. Based on these results, we concluded that poplar grown in the Saemangeum land reclamation project area is not only useful for its biomass and energy production, but also suitable to be a carbon sink for GHG mitigation.

4.2. Potential Impact of Microclimate on Photosynthetic Parameters

Interestingly, the net height growth of poplar seedlings is rapidly increased in the second rotation (14W) compared with first rotation (13W), but that of seedlings in the third rotation (15D) was significantly decreased (Figure 2) ($p \leq 0.05$). Based on the volumetric soil moisture content, we classified climatic conditions into two types (moderate (13W, 14W) and drought (15D)). Changes in tree volume are often inferred from DBH and tree height increment, which can have important implications for the accuracy of predictions [77]. Increment is more physiologically related to size than chronological age in environmental stress-related conditions [78]. On top of that, height increment is more dependent on differences in genetics and environmental conditions, while diameter increment is more closely related to the current amount of foliage and tree competitive status [79]. In this study, chlorophyll and carotenoid contents of poplar were sensitive to recent drought in SRC. Moreover, important changes were observed for chlorophyll a/b ratio under drought (15D) with decrease in the ratio during the growing season (June) and post-growing season (October) compared with the previous year (14W) at site 2012. However, there was no decrease pattern in site 2013 after drought. These changes in ratio act as a defensive mechanism in order to enhance photosynthetic efficiency against photo-inhibition [80]. In general, the a/b ratio is reduced over 65% in stress condition, because of contributing to the enlargement of the PS II antenna size, enhancing chlorophyll b contents [81]. In many studies, reduced photosynthetic pigments were an adaption of the plant to protect itself from photo-inhibition and photodynamic damage in response to the drought [82,83]. According to the results of Lang et al. [84], photosynthetic efficiency was restricted by photoinhibition but can be limited

by enhancing photorespiration and heat dissipation (Tables 10 and 11). To avoid photoinhibition and enhance photosynthetic efficiency, plants reduce the size of their chlorophyll antennae in their photosystems and their chlorophyll content in response to the drought [85,86]. Based on a field study of chlorophyll fluorescence, our previous data also showed a declined pattern of chlorophyll fluorescence of poplar seedling in the Saemangeum area of Korea during the drought, indicating no minimization of the antenna size on changes in the specific energy fluxes per reaction in poplar during drought (data not shown). In the same context, in our study, the total Chl, Chl a/b, and Car contents significantly decreased as the drought intensity increased (Figure 2, Table 10). Many studies have indicated that reduced photosynthetic pigments are tree physiological adaptations that plants use to protect themselves from photoinhibition and photodynamic damage [83]. The decreased Chl a/b indicates damage to the light-harvesting complex [87,88]. According to the result of Lei et al. [89], the reduced Car content indicates that the relative water deficit in this study might have induced oxidative stress via the accumulation of reactive oxygen species. However, the decrease in the Chl T/Car during the drought indicates that the amount of Car increased compared to the Chl T in response to drought, because carotenoids play an important role as a lipid soluble antioxidant, a precursor in signaling and as an accessory pigment to protect photochemical process and change under the drought or water-deficit, Car affects water deficit tolerance of trees [90]. Weissert et al. [91] reported the photosynthetic CO_2 uptake potential of tree species across seasons. Mean net photosynthetic capacities across all seasons were closely related to tree C sequestration rates, suggesting that increased photosynthesis enhances growth rates and therefore tree C sequestration rates. However, it is still required to investigate tree C potential in oceanic climates such as the Saemangeum region, because little is known about photosynthetic CO_2 uptake [91,92].

In our study, the survival rate of *Populus* × *Canadensis* Moench. was not affected by meteorological changes in the study area (data not shown). However, different responses to the distinct water deficit intensities in dissimilar seasons were observed. To balance carbon fixing and water containment during the drought, the plants demonstrated a trade-off between growth and physiological responses [93]. These results remain a challenge to investigate how these physiological changes affect sustainable biomass yield and whether poplar trees can grow and their biomass regardless of these meteorological events.

4.3. Successional Patterns in Flora on SRC

Kim et al. [15] reported that the distribution of glycophyte (82.6%, 95 species) is higher than that of halophyte (17.4%, 20 species) in Saemangeum reclaimed land. Moreover, we explored flora distribution on SRC and its neighboring vegetation throughout 2013, 2014 and 2015. The Saemangeum area has been transformed into a different environment from the existing tidal flat ecosystem due to reclamation. Generally, *P. communis* Trin. (halophyte) and other herbaceous plants grown in tidal flat are dominant in the reclaimed land in South Korea [94], but other dominant plants might be formed in the understory vegetation formed after afforestation of the short rotation coppices, because of the shade effect [13]. Birmele et al. [95] reported that the neighboring ground vegetation on SRC had a dominant tendency in light-demanding plant species. However, their proposition can be deteriorated from 62 to 39%, steadily over time, whereas the proposition of semi-shade species shows an increase from 22 to 34% as SRC trees change canopy levels. In SRC 2012, the dominant plant species changed gradually in the second (14W) and third rotation (15D), and neighboring vegetation of SRC was also changed. Initially, *A. subulatus* Michx. (glycophyte) was the dominant species in the first rotation (13W), and species composition was changed by *S. viridis* (halophyte). Meanwhile, Li et al. [96] reported halophyte species in our study site—*S. viridis* is known as a dominant annual in sandy land, and is known as a good candidate for vegetation restoration initiatives, especially in soil drought conditions [97]. Kim [98] reported that the indicator herbaceous plants in reclaimed land is divided among 45 plants normally. In the initial stage of reclamation, *Suaeda japonica* achieved a dominant position as a pioneer halophyte, because it usually lives in a pedosphere with T-N (0.22–0.31) and P_2O_5 (0.056–0.076) with high salinity

(Na 7.22–7.36; Cl 9.27–10.90). *A. subulatus* Michx, the species found in our site, usually lives in a pedosphere with T-N (0.69–1.02) and P_2O_5 (0.074) with moderate salinity (Na 1.98; Cl 2.37). In addition, *P. communis* Trin., known as halophyte, lives in T-N (0.47–0.53) and P_2O_5 (0.039–0.041) with moderate salinity (Na 0.41–0.71; Cl 0.47–1.35). It was found that halophyte distribution in SRC can be interpreted as resalinization temporarily, but more long-term monitoring and additional studies will be required to predict this precisely.

Monitoring the plant diversity in the area surrounding the SRC showed that the dominant species in the Saemangeum land reclamation area changed in their species composition over three years. Birmele et al. [95] reported that high soil moisture and irrigated SRC plots might affect the high water ability of neighboring plants and impact species richness on successional changes in photodiversity of SRC, increasing the species number. In 2013, the dominant species in the SRC was identified to be *S. viridis*, but *Sonchus brachyotus* and *C. epigeios* also increased in 2014 (second rotation of the SRC). Overall, poplar afforestation on reclaimed land changed the plant species diversity (frequency, density and number of species) (Tables 7–9). Oh and Choi [99] reported that in reclaimed land, the occurrence of *C. epigeios* and *Sonchus brachyotus* is an intermediate step between desalination and vegetational succession. The influence of plant succession on the distribution of *S. viridis*, *Sonchus brachyotus*, and *C. epigeios* may be related to the desalinization of the soil of reclaimed land. Yeo et al. [58] reported that if a superior species or clone, which has a high transpiration rate, is planted on reclaimed land for revegetation, the soil salinity level could be alleviated, preventing an increase in salinity level through the capillary tube over time. The change in the plant communities in the Saemangeum area appeared to be affected by the degree of desalination of the reclaimed soil. However, even if the soil organic matter is the lowest in SRC2014 amongst other sites, which means a less changed site in succession of phytodiversity, we did not find a correlation between the number of halophytes and soil organic matter in our site (data not shown). Moreover, our results still remain statistically significant for a short-rotation forest in the Saemangeum area whether or not the low level of salinity in the soil was related to the progress in vegetational succession from reclaimed land. Therefore, it is required to understand how vegetation on reclaimed land changes the soil chemical properties through further research, and is recommended to monitor successional changes to phytodiverity in SRCs in reclaimed land, aside from biomass yield monitoring.

5. Conclusions

Our study showed an unprecedented study result on SRC bioenergy production via reclaimed land, having two significant findings for short rotation coppice in Saemangeum reclaimed land. Firstly, in this study, *Populus* × *Canadensis* Moench. in the SRC of the Saemangeum land reclamation area has huge potential for GHG mitigation via carbon storage and for yielding biomass to produce raw material for generating bioenergy. Furthermore, *Populus* × *Canadensis* Moench. grown this area scored third grade (G3) in the Korean wood pellet specification, indicating that *Populus* × *Canadensis* Moench. grown here can contribute to the sustainable production of bioenergy. The biomass yield per area of poplar grown was calculated to be 13.5 oven dry tons ha^{-1} $year^{-1}$, and the carbon stock and CO_2 absorption volume were estimated to be 6.2 Mg C ha^{-1} $year^{-1}$ and 22.9 Mg CO_2 ha^{-1} $year^{-1}$, respectively. Nevertheless, future studies are clearly needed to further understand the effects of long-term monitoring on carbon storage potential, such as climate change projection scenario analysis, growth patterns and carbon storage of belowground and aboveground of *Populus* in the Saemangeum area. Second, in terms of microclimate, this is the only study quantifying the amount of flora distribution in coastal reclaimed SRCs during temporary drought, especially in the Saemangeum area. Our findings suggest that halophyte distribution and soil nutrients in afforested areas of reclaimed land can be changed during drought, changing its soil moisture condition over time. Although our findings of the total biomass production and carbon sequestration are valuable for SRC management, further sustainable management will also be required to operate domestic bioenergy production and carbon credit as appears by decrease in net growth, photosynthetic pigment and gas exchange fluxes of

poplar seedlings growing coastal reclaimed land. Therefore, sustainable management, yield modeling, and long-term monitoring of the Saemangeum SRC are necessary to mitigate GHGs and produce green energy in Korean peninsula. In addition, these results suggest that current strategies of short rotation forest management in marginal areas, such as the Saemangeum land reclamation project area, should be steadily monitored and improved to minimize the forest decline in afforested areas by restoring the indigenous or halophyte vegetation of reclaimed land, monitoring vegetation succession as well.

Author Contributions: J.J. and S.Y.W. conceptualize, designed this study and then wrote the manuscript; J.J., M.J.K., S.M.J., I.R.K. and J.K.L. performed the field experiments; J.J. analyzed the accumulated data; S.Y.W. developed the conceptualization, funding acquisition and contributed analysis tools. All authors have read to the published version of the manuscript and agreed with extent of contribution.

Funding: This research was funded by Korea Forest Service (Korea Forestry Promotion Institute), Republic of Korea, grant number 2018120B10-2020-AB01 and The APC was funded by Korea Forest Service (Korea Forestry Promotion Institute).

Acknowledgments: This study was carried out with the support of 'The R&D Program for Forest Science Technology through the Korea Forest Service (Korea Forestry Promotion Institute), Grant No. 2018120B10-2020-AB01'. We are grateful to team of Urban Environment and Plant Science Lab., and to field director and forester of Western Regional Office of Korea Forest Service and Jeongeup National Forest Station who helped with the field survey.

Conflicts of Interest: The authors declare no conflict of interest.

Appendix A

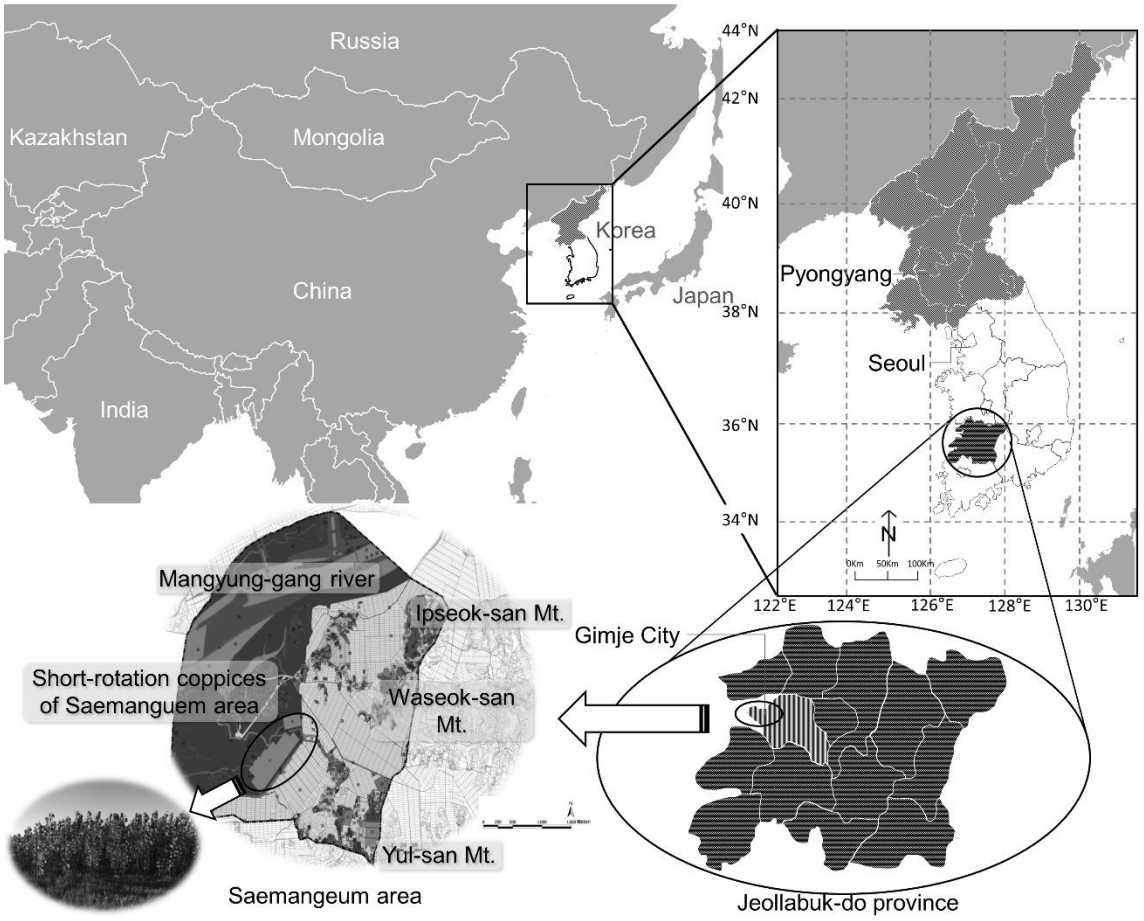

Figure A1. Site description of short rotation coppice in Saemangeum reclaimed land, South Korea.

Appendix B

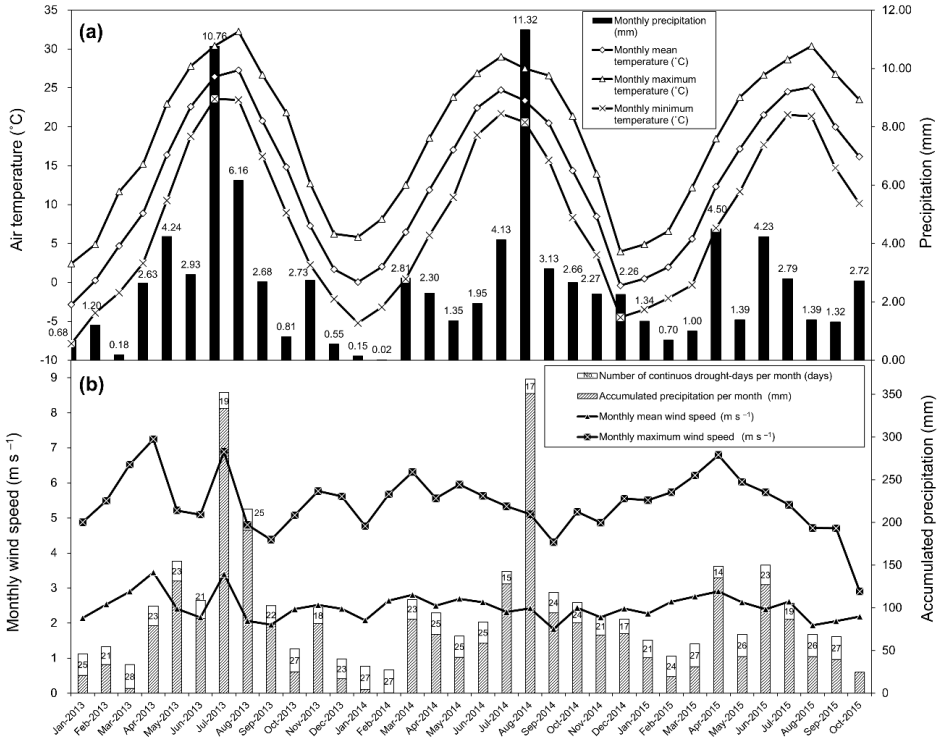

Figure A2. Weather condition of short rotation coppice in Saemangeum reclaimed land, South Korea. (**a**) Monthly air temperature and precipitation; (**b**) monthly wind speed, continuous drought days per month (which means the day recorded 0 mm precipitation for 24 h based on database from Korea Meteorological Administration) and accumulated precipitation for the study site throughout 2013, 2014 and 2015.

Appendix C

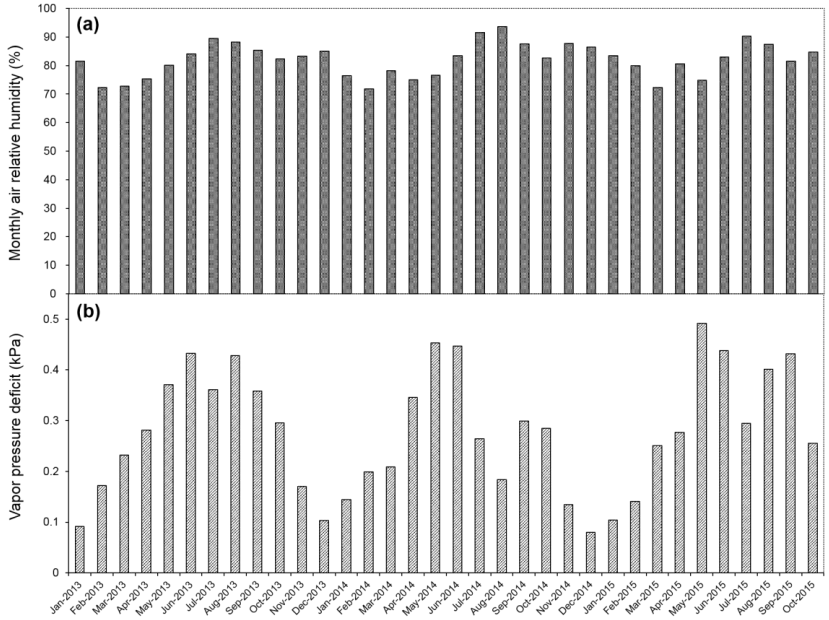

Figure A3. Weather condition of short rotation coppice in Saemangeum reclaimed land, South Korea. (**a**) Relative humidity; (**b**) vapor pressure deficit for the study site throughout 2013, 2014 and 2015.

Appendix D

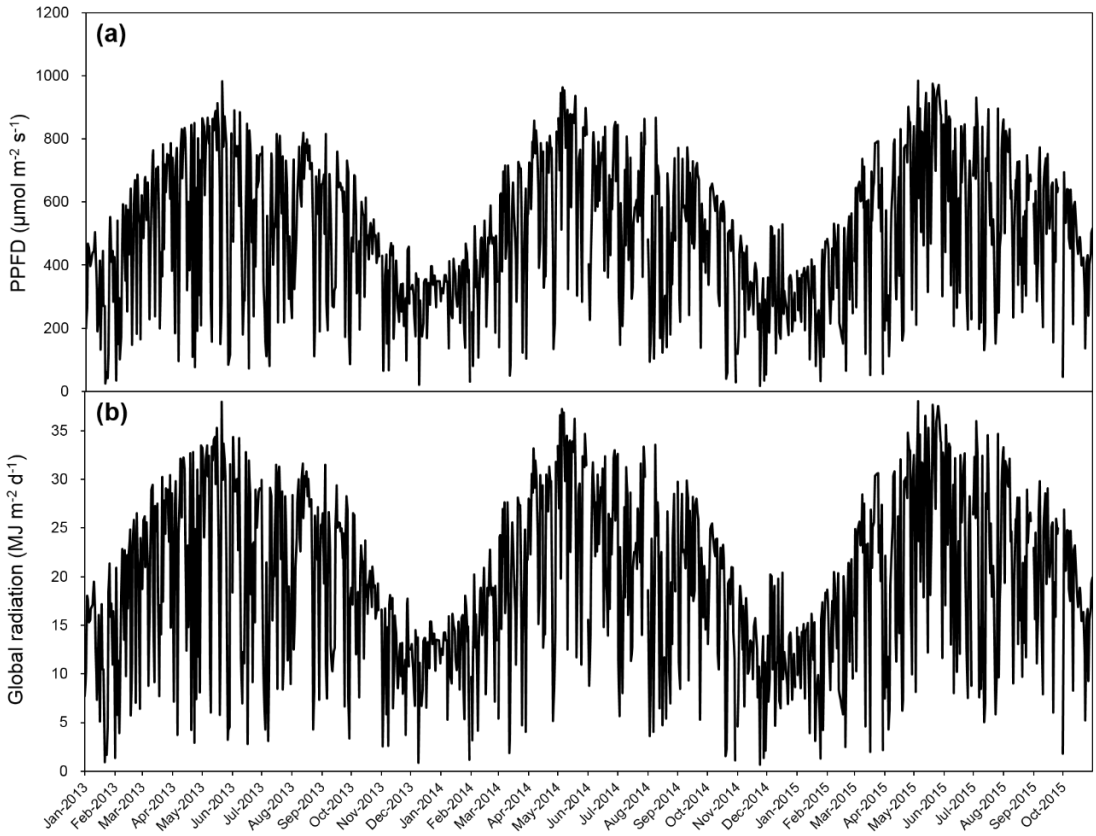

Figure A4. Weather condition of short rotation coppice in Saemangeum reclaimed land, South Korea. (**a**) Photosynthetic photon flux density; (**b**) global radiation for the study site throughout 2013, 2014 and 2015.

Appendix E

Table A1. Specifications for Korean wood pellet quality criteria according to National Institute of Forest Science standard specification (KR), Pellet Fuels Institute standard (US), and EN-Plus standard (EU) [29].

Specification.		*Q* ≥(MJ kg^{-1})	Ash	N	Cl	S	As	Cd	Cr	Cu	Pb	Hg	Ni	Zn
			≤(%)				≤(mg kg^{-1})							
KR	G1	18.0	0.7	0.3	0.05	0.05	1.0	0.5	10	10	10	0.05	10	100
	G2		1.5	0.5										
	G3	16.9	3.0	0.7										
	G4		6.0	1.0										
US	P	NA	1.0	NA	0.03	NA								
	S		2.0	NA										
	U		6.0	NA										
EU	A1	16.64	0.7	0.3	0.02	0.04	1.0	0.5	10	10	10	0.1	10	100
	A2		1.2	0.5		0.05								
	B		2.0	1.0	0.03									

KR, Republic of Korea; US, United States of America; EU, European Union. G1, first grade; G2, second grade; G3, third grade; G4, fourth grade [43]; P, PFI Premium; S, PFI Standard; U, PFI Utility [44]; A1, EN-Plus-A1; A2, EN-Plus-A2; B, EN-Plus-B [45]; NA, no value has been established.; *Q*, net calorific value; Ash, ash content.

References

1. FAO. *Global Forest Resources Assessment 2010: Specifications of National Reporting Tables for FRA 2010*; Forest Resources Assessment Programme; United Nations Food and Agricultural Organization: Rome, Italy, 2007; p. 135.
2. UNFF. United Nations Forum on Forests. 2018. Available online: http://www.un.org/esa/forests/index.html (accessed on 5 November 2016).
3. Etienne, X.L.; Yu, J. Inverse price spread and illiquid trading in Korea-ETS. *Carbon Manag.* **2017**, *8*, 1–11. [CrossRef]
4. Lee, J.I. *A Study on the Energy Utilization of Woody Biomass*; Gyeonggi Research Institute: Suwon, Korea, 2009; pp. 9–74. (In Korean)
5. Lee, J.C.; Kang, K.Y. Analyses of GHG reduction effectiveness and economic feasibility in the wood pellet fuel switching project. *J. Korean Wood Sci. Technol.* **2013**, *41*, 594–605. [CrossRef]
6. McAlpine, R.G.; Brown, C.L.; Herrick, A.M.; Ruark, H.E. Silage sycamore. *Forest Farmer* **1966**, *26*, 6–7.
7. Herrick, A.M.; Brown, C.L. A new concept in cellulose production-silage sycamore. *Agr. Sci. Rev.* **1967**, *5*, 8–13.
8. Schreiner, E.J. *Mini-Rotation Forestry*; USDA Forest Service Research: Madison, WI, USA, 1970; p. 32.
9. Zsuffa, L. Hybrid poplar pulpwood production trials in South-eastern Ontario. *For. Chron.* **1973**, *49*, 125. [CrossRef]
10. Hyun, Y.I.; Kim, J.H.; Han, Y.C.; Lee, K.J. Wood biomass production of twelve tree species in coppice plantations managed under 1-, 2- and 3- year rotations. *J. Korean For. Soc.* **1982**, *55*, 30–36, (In Korean with English abstract).
11. Kim, H.C.; Yeo, J.K.; Koo, Y.B.; Shin, H.N.; Choi, J.Y.; Lee, H.H. Growth and biomass production of fast growing tree species treated with slurry composting and biofiltration liquid fertilizer. *Korean J. Soil Sci. Fertil.* **2011**, *44*, 206–214, (In Korean with English abstract). [CrossRef]
12. Park, P.S.; Kim, K.Y.; Jang, W.S. Comparison of seedling survival rate and growth among 8 different tree species in Seosan reclamation area. *J. Korean For. Soc.* **2009**, *98*, 496–503, (In Korean with English abstract).
13. Lee, S.W.; Cheon, B.H.; Woo, S.Y.; Kim, K.H.; Han, B.H.; Jang, J.H.; Kim, J.Y.; Oh, J.S.; Kwak, M.J.; Lee, T.Y.; et al. *Monitoring for Wood Biomass Production and Environmental Effect of Short Rotation Coppice Culture in Saemangeum Reclaimed Land*; Korea Forest Service: Daejeon, Korea, 2015; pp. 147–166. (In Korean)
14. Kaminska, A. Method for increasing the calorific value of fragmented wood biomass. *Tech. Trans.* **2011**, *108*, 97–105.
15. Isebrands, J.G.; Karnosky, D.F. Environmental benefits of poplar culture. In *Poplar Culture in North America*; Dickmann, D.I., Isebrands, J.G., Eckenwalder, J.E., Richardson, J., Eds.; NRC Research Press: Ottawa, Canada, 2001; pp. 207–218.
16. Westphal, L.M.; Isebrands, J.G. *Phytoremediation of Chicago's Brownfields: Consideration of Ecological Approaches and Social Issues, in Brownfields Proc*; North Central Research Station: Chicago, IL, USA, 2001; pp. 1–9.
17. Kim, C.H.; Choi, J.H.; Lee, K.B.; Kim, H.K.; Lee, N.S. A Study on the flora and life form of the western coast reclaimed land in Korea. *J. Korean Isl. Stud.* **2013**, *25*, 213–226. (In Korean)
18. Yoon, S.K.; Park, E.J.; Choi, Y.I.; Bae, E.K.; Kim, J.H.; Park, S.Y.; Kang, K.S.; Lee, H. Responses to drought and salt stress in leaves of poplar (*Populus alba* × *Populus glandulosa*): Expression profiling by oligonucleotide microarray analysis. *Plant Physiol. Biochem.* **2014**, *84*, 158–168. [CrossRef] [PubMed]
19. Korea Meteorological Administration National Climate Data Service System. Available online: https://data.kma.go.kr/tmeta/stn/selectStnDetail.do (accessed on 5 December 2017).
20. Chaves, M.M.; Maroco, J.P.; Pereira, J.S. Understanding plant responses to drought—From genes to the whole plant. *Funct. Plant Biol.* **2003**, *30*, 239–264. [CrossRef] [PubMed]
21. Yordanov, I.; Velikova, V.; Tsonev, T. Plant responses to drought, acclimation, and stress tolerance. *Photosynthetica* **2000**, *38*, 171–186. [CrossRef]
22. Ferdousee, N.; Kabir, A.; Ahmed, R.; Kwon, M.; Hoque, A.R.; Mohiuddin, M.; Kim, W. Water stress effects on *Dipterocarpus turbinatus* seedlings. *For. Sci. Technol.* **2010**, *6*, 18–23. [CrossRef]
23. Schlesinger, W.H.; Dietze, M.C.; Jackson, R.B.; Phillips, R.P.; Rhoades, C.C.; Rustad, L.E.; Vose, J.M. Forest biogeochemistry in response to drought. *Glob. Change Biol.* **2016**, *22*, 2318–2328. [CrossRef]

24. Salinger, M.J.; Griffiths, G.M. Trends in New Zealand daily temperature and rainfall extremes. *Int. J. Climatol.* **2001**, *21*, 1437–1452. [CrossRef]
25. Macinnis-Ng, C.; Schwendenmann, L. Litterfall, carbon and nitrogen cycling in a southern hemisphere conifer forest dominated by kauri (*Agathis australis*) during drought. *Plant Ecol.* **2015**, *216*, 247–262. [CrossRef]
26. Kim, Y.H.; Kim, M.K.; Lee, W.S. An investigation of large-scale climate indices with the influence on temperature and precipitation variation in Korea. *Atmosphere* **2008**, *18*, 83–95, (In Korean with English abstract).
27. Wang, H.; He, S. The north China/northeastern Asia severe summer drought in 2014. *J. Clim.* **2015**, *28*, 6667–6681. [CrossRef]
28. Porteous, A.; Mullan, B. *The 2012–2013 Drought: An Assessment and Historical Perspective*; MPI Tech Paper; Ministry for Primary Industries, National Institute of Water and Atmospheric Research: Wellington, New Zealand, 2013; p. 57.
29. Clark, A.; Tait, A. *Drought, Agricultural Production and Climate Change: A Way Forward to a Better Understanding*; Client Report WLG2008-33; National Institute of Water and Atmosphere: Wellington, New Zealand, 2008.
30. Lee, K.B.; Xu, M.; Kim, J.D.; Jung, K.Y. Soil characteristics and utilization on reclaimed land in Jangsu Province coastal region of China. *J. Korean Soc. Int. Agric.* **2006**, *18*, 245–252, (In Korean with English abstract).
31. Jang, J.H.; Woo, S.Y.; Kim, S.H.; Inkyin, K.; Kwak, M.J.; Lee, H.K.; Lee, T.Y.; Lee, W.Y. Effect of increased soil fertility and plant growth promoting rhizobacteria inoculation on biomass yield, energy value and physiological response of poplar in short rotation coppices in a reclaimed tideland: A case study in Saemangeum area of Korea. *Biomass Bioenerg.* **2017**, *107*, 29–38. [CrossRef]
32. Kim, D.; Kim, M.; Kim, M.; Park, K. Improvement of Saemangeum dredged soils using coffee sludge for vegetation soil. *Adv. Mater. Sci. Eng.* **2016**, 1–11. [CrossRef]
33. Suh, K.H. Using sunshine duration to estimate photosynthetic photon flux density at Taegu, Korea. *Korean J Ecol.* **1996**, *19*, 65–70, (In Korean with English abstract).
34. Shin, H.N.; Kim, H.C.; Kang, K.S.; Lee, J.C. Differences in biomass production by rotation interval and planting density in short-rotation Forestry. In Proceedings of the Annual Forestry Conference of Korean Society of Forest Science, Jeju, Korea, 8 February 2012; Korean Society of Forest Science: Seoul, Korea, 2012.
35. Makkonen, K.; Helmisaari, H.S. Seasonal and yearly variations of fine-root biomass and necromass in a Scots pine (*Pinus sylvestris* L.) stand. *For. Ecol. Manage.* **1998**, *102*, 283–290. [CrossRef]
36. Caims, M.A.; Brown, S.; Helmer, E.H.; Baumgrardner, G.A. Root biomass allocation in the world's upland forests. *Oecologia* **1997**, *111*, 1–11. [CrossRef]
37. Noh, N.J.; Son, Y.H.; Kim, J.S.; Kim, R.H.; Seo, K.Y.; Seo, K.W.; Koo, J.W.; Kyung, J.H.; Park, I.H.; Lee, Y.J.; et al. A Study on Estimation of Biomass, Stem Density and Biomass Expansion Factor for Stand Age Classes of Japanese Larch (*Larix leptolepis*) Stands in Gapyeong Area. *J. Korean For. BioEnergy* **2006**, *25*, 1–8, (In Korean with English abstract).
38. Han, J.S. A Study on Planting Management Method for Enlargement and Quality of CO_2 Uptake by Tree in the Landfill Site of Metropolitan Area, Korea. Master's Thesis, University of Seoul, Seoul, Korea, 2008. (In Korean with English abstract)
39. Ovington, J.D. The composition of tree. *Forestry* **1956**, *29*, 22–29. [CrossRef]
40. Reichle, D.E.; Dinger, B.E.; Edward, N.T.; Harris, W.F.; Sollins, P. Carbon flow and storage in a forest ecosystem. In *Carbon and the Biosphere*; Woodwell, G.M., Pecan, E.V., Eds.; US Atom Energy Commiss, Office of Information Services: Upton, NY, USA, 1973; pp. 345–365.
41. Ajtay, G.L.; Ketner, P.; Duvigneaus, P. *Terrestrial Production and Phytomass*, 1st ed.; John Wiley & Sons: Chichester, UK, 1979; pp. 129–181.
42. Chow, P.; Rolfe, G.L. Carbon and hydrogen contents of short rotation biomass of five hardwood species. *Wood Fiber Sci.* **1989**, *21*, 30–36.
43. Jo, H.K. Carbon uptake and emissions in urban landscape, and the role of urban greenspace for several cities in Kangwon province. *J. Korean Inst. Landsc. Archit.* **1999**, *27*, 39–53. (In Korean)
44. Braun-Blanquet, J. *Plant Sociology: Basics of Vegetation Science*; Springer: Berlin, Germany, 1965; p. 865.
45. Taylor, H.C. A vegetation survey of the Cape of Good Hope nature reserve. I. The use of association-analysis and Braun-Blanquet methods. *Bothalia* **1984**, *15*, 245–258. [CrossRef]
46. National Institute of Forest Science. *Specifications and Quality Standards of Wood Products*; National Institute of Forest Science: Seoul, Korea, 2015; pp. 98–99. (In Korean)

47. Pellet Fuels Institute. *Pellet Fuels Institute Standard Specification for Residential/Commercial Densified Fuel QA/QC Handbook*; Pellet Fuels Institute: Arlington, VA, USA, 2011; p. 13.
48. European Pellet Council. Part 3: Pellet quality requirements. In *EN Plus Handbook*; European Pellet Council: Brussels, Belgium, 2015; p. 7.
49. Zhao, M.; Running, S.W. Drought-induced reduction in global terrestrial net primary production from 2000 through 2009. *Science* **2010**, *329*, 940–943. [CrossRef] [PubMed]
50. Kung, H.Y.; Hua, J.S.; Chen, C.T. Drought forecast model and framework using wireless sensor networks. *J. Inf. Sci Eng.* **2006**, *22*, 751–769.
51. Bremner, J.M. Chemical methods. In *Methods of Soil Analysis*; Soil Science Society of America and American Society of Agronomy: Madison, WI, USA, 1966; pp. 85–1122.
52. Allison, L.E. Agronomy Monograph 9. In *Methods of Soil Analysis: And Chemical and Microbiological Properties*; Black, C.A., Ed.; American Society of Agronomy: Madison, WI, USA, 1965; pp. 1367–1378.
53. Bray, R.H.; Kurtz, L.T. Determination of total organic and available forms of phosphorus in soils. *Soil Sci.* **1945**, *59*, 39–45. [CrossRef]
54. Arnon, D.I. Copper enzymes in isolated chloroplasts. polyphenoloxidase in Beta vulgaris. *Plant Physiol.* **1949**, *24*, 1–15. [CrossRef] [PubMed]
55. Pingrey, D.W. *Forest Products Energy Overview: Energy and Wood Products Industry*; Forest Products Research Society: Madison, WI, USA, 1976; pp. 1–14.
56. Duca, D.; Riva, G.; Pedretti, E.F.; Toscano, G. Wood pellet quality with respect to EN 14961-2 standard and certifications. *Fuel* **2014**, *135*, 9–14. [CrossRef]
57. Fernandez, M.J.; Barro, R.; Perez, J.; Losada, J.; Ciria, P. Influence of the agricultural management practices on the yield and quality of poplar biomass (a 9-year study). *Biomass Bioenerg.* **2016**, *93*, 87–96. [CrossRef]
58. Yeo, J.K.; Shin, H.N.; Kim, H.C.; Woo, K.S. Growth characteristics and adaptability of three-year-old poplar clones in a reclaimed tidal flat. *J. Agricult. Life Sci.* **2011**, *45*, 17–23.
59. Klasnja, B.; Kopitovic, S.; Orlovic, S. Wood and bark of some poplar and willow clones as fuelwood. *Biomass Bioenerg.* **2002**, *23*, 427–432. [CrossRef]
60. Yeo, J.K.; Woo, K.S.; Koo, Y.B.; Kim, Y.S. Growth performance and adaptability of three-year-old poplar and willow clones in a riparian area. *J. Korean Soc. Environ. Res. Technol.* **2007**, *10*, 40–50.
61. Koo, Y.B.; Yeo, J.K. The status and prospect of poplar research in Korea. *J. Korea For. Energy* **2003**, *22*, 1–17.
62. Manzone, M.; Calvo, A. Energy and CO_2 analysis of poplar and maize crops for biomass production in north Italy. *Renew. Energy* **2016**, *86*, 675–681. [CrossRef]
63. Oliveira, N.; Rodríguez-Soalleiro, R.; Pérez-Cruzado, C.; Cañellas, I.; Sixto, H.; Ceulemans, R. Above-and below-ground carbon accumulation and biomass allocation in poplar short rotation plantations under Mediterranean conditions. *For. Ecol. Manag.* **2018**, *428*, 57–65. [CrossRef]
64. Kim, H.C.; Lee, S.J.; Lee, W.Y.; Kang, J.W. Selection of poplar clones for short rotation coppice in a riparian area. *J. Korean For. Soc.* **2016**, *105*, 103–107, (In Korean with English abstract).
65. Kim, H.C.; Shin, H.; Lee, H.H.; Yeo, J.K.; Kang, K.S. Growth response and adaptability of poplar species treated with liquid pig manure. *J. Korean For. Soc.* **2013**, *102*, 420–427, (In Korean with English abstract).
66. Son, Y.M.; Kim, R.H.; Kang, J.T.; Lee, K.S.; Kim, S.W. A practical application and development of carbon emission factors for 4 major species of warm temperate forest in Korea. *J. Korean For. Soc.* **2014**, *103*, 593–598, (In Korean with English abstract). [CrossRef]
67. Osuna, J.L.; Baldocchi, D.D.; Kobayashi, H.; Dawson, T.E. Seasonal trends in photosynthesis and electron transport during the Mediterranean summer drought in leaves of deciduous oaks. *Tree Physiol.* **2015**, *35*, 485–500. [CrossRef]
68. Lawlor, D.W.; Tezara, W. Causes of decreased photosynthetic rate and metabolic capacity in water-deficient leaf cells: A critical evaluation of mechanisms and integration of processes. *Ann. Bot.* **2009**, *103*, 561–579. [CrossRef]
69. Sekhar, K.M.; Reddy, K.S.; Reddy, A.R. Amelioration of drought-induced negative responses by elevated CO_2 in field grown short rotation coppice mulberry (*Morus* spp.), a potential bio-energy tree crop. *Photosynth. Res.* **2017**, *132*, 151–164. [CrossRef]
70. Fabio, E.S.; Smart, L.B. Effects of nitrogen fertilization in shrub willow short rotation coppice production–a quantitative review. *GCB Bioenergy* **2018**, *10*, 548–564. [CrossRef]

71. Schweier, J.; Molina-Herrera, S.; Ghirardo, A.; Grote, R.; Díaz-Pinés, E.; Kreuzwieser, J.; Haas, E.; Butterbach-Bahl, K.; Rennenberg, H.; Schnitzler, J.-P.; et al. Environmental impacts of bioenergy wood production from poplar short-rotation coppice grown at a marginal agricultural site in Germany. *GCB Bioenergy* **2017**, *9*, 1207–1221. [CrossRef]
72. San Miguel, G.; Corona, B.; Ruiz, D.; Landholm, D.; Laina, R.; Tolosana, E.; Sixto, H.; Cañellas, I. Environmental, energy and economic analysis of a biomass supply chain based on a poplar short rotation coppice in Spain. *J. Clean. Prod.* **2015**, *94*, 93–101. [CrossRef]
73. Kwon, K.C.; Lee, D.K. Above- and below-ground biomass and energy content of *Quercus mongolica*. *J. Korean For. Energy* **2006**, *25*, 31–38.
74. Ovington, J.D. Quantitative ecology and the woodland ecosystem concept. *Adv. Ecol. Res.* **1962**, *1*, 103–192.
75. Santatonio, D. Processing modeling of forest growth responses to environmental stress. In *Modeling Growth and Production of Tree Roots*; Dickson, R.K., Meldah, R.S., Ruark, G.A., Warren, W.G., Eds.; Timber Press: Portland, OR, USA, 1990; pp. 124–141.
76. Myung, S.Y.; Eon, Y.J.; Dong, J.I.; Park, Y.K.; Kang, B.S.; Jeon, J.K. Characteristics of thermal decomposition of major components of biomass isolated from wood. *J. Korean Ind. Eng. Chem.* **2004**, *15*, 896–900.
77. Hann, D.W.; Weiskittel, A.R. Evaluation of alternative approaches for predicting individual tree volume increment. *West J. Appl. For.* **2010**, *25*, 120–126. [CrossRef]
78. Bond, B.J.; Czarnomski, N.M.; Cooper, C.; Day, M.E.; Greenwood, M.S. Developmental decline in height growth in Douglas-fir. *Tree Physiol.* **2007**, *27*, 441–453. [CrossRef]
79. Ritchie, M.W.; Hamann, J.D. Individual-tree height-, diameter-and crown-width increment equations for young Douglas-fir plantations. *New For.* **2008**, *35*, 173–186. [CrossRef]
80. Anjum, S.A.; Xie, X.Y.; Wang, L.C.; Saleem, M.F.; Man, C.; Lei, W. Morphological, physiological and biochemical responses of plants to drought stress. *Afr. J. Agric. Res.* **2011**, *6*, 2026–2032. [CrossRef]
81. Masuda, T.; Tanaka, A.; Melis, A. Chlorophyll antenna size adjustments by irradiance in *Dunaliella salina* involve coordinate regulation of chlorophyll a oxygenase (CAO) and *Lhcb* gene expression. *Plant Mol. Biol.* **2003**, *51*, 757–771. [CrossRef]
82. Lei, Y.; Yin, C.; Li, C. Differences in some morphological, physiological, and biochemical responses to drought stress in two contrasting populations of *Populus przewalskii*. *Physiol. Plantarum* **2006**, *127*, 182–191. [CrossRef]
83. Karataş, İ.; Öztürk, L.; Demir, Y.; Ünlükara, A.; Kurunç, A.; Düzdemir, O. Alterations in antioxidant enzyme activities and proline content in pea leaves under long-term drought stress. *Toxicol. Ind. Health* **2014**, *30*, 693–700. [CrossRef]
84. Lang, Y.; Wang, M.; Zhang, G.C.; Zhao, Q.K. Experimental and simulated light responses of photosynthesis in leaves of three tree species under different soil water conditions. *Photosynthetica* **2013**, *51*, 370–378. [CrossRef]
85. Jiang, Y.; Huang, B. Osmotic adjustment and root growth associated with drought preconditioning-enhanced heat tolerance in Kentucky bluegrass. *Crop Sci.* **2001**, *41*, 1168–1173. [CrossRef]
86. Wang, Y.; Xu, C.; Wu, M.; Chen, G. Characterization of photosynthetic performance during reproductive stage in high-yield hybrid rice LYPJ exposed to drought stress probed by chlorophyll a fluorescence transient. *Plant Growth Regul.* **2017**, *81*, 489–499. [CrossRef]
87. Sfichi-Duke, L.; Ioannidis, N.E.; Kotzabasis, K. Fast and reversible response of thylakoid-associated polyamines during and after UV-B stress: A comparative study of the wild type and a mutant lacking chlorophyll b of unicellular green alga *Scenedesmus obliquus*. *Planta* **2008**, *228*, 341. [CrossRef] [PubMed]
88. Sato, R.; Ito, H.; Tanaka, A. Chlorophyll b degradation by chlorophyll b reductase under high-light conditions. *Photosynth. Res.* **2015**, *126*, 249–259. [CrossRef]
89. Lei, S.; Yunzhou, Q.; Fengchou, J.; Changhai, S.; Chao, Y.; Yuxin, L.; Mengyu, L.; Baodi, D. Physiological mechanism contributing to efficient use of water in field tomato under different irrigation. *Plant Soil Environ.* **2009**, *55*, 128–133. [CrossRef]
90. Jaleel, C.A.; Manivannan, P.; Wahid, A.; Farooq, M.; Al-Juburi, H.J.; Somasundaram, R.; Panneerselvam, R. Drought stress in plants: A review on morphological characteristics and pigments composition. *Int. J. Agric. Biol.* **2009**, *11*, 100–105.
91. Weissert, L.F.; Salmond, J.A.; Schwendenmann, L. Photosynthetic CO_2 uptake and carbon sequestration potential of deciduous and evergreen tree species in an urban environment. *Urban Ecosyst.* **2017**, *20*, 663–674. [CrossRef]

92. Yilmaz, D.; Cannavo, P.; Séré, G.; Vidal-Beaudet, L.; Legret, M.; Damas, O.; Peyneau, P.E. Physical properties of structural soils containing waste materials to achieve urban greening. *J. Soils. Sediments* **2018**, *18*, 442–455. [CrossRef]
93. Fernàndez, R.J.; Reynolds, J.F. Potential growth and drought tolerance of eight desert grasses: Lack of a trade-off? *Oecologia* **2000**, *123*, 90–98. [CrossRef] [PubMed]
94. Kim, E.K. *Halophytes of Korea*; Nature and Ecology: Seoul, Korea, 2013; pp. 331–368. (In Korean)
95. Birmele, J.; Kopp, G.; Brodbeck, F.; Konold, W.; Sauter, U.H. Successional changes of phytodiversity on a short rotation coppice plantation in Oberschwaben, Germany. *Front. Plant Sci.* **2015**, *6*, 124. [CrossRef] [PubMed]
96. Li, F.R.; Zhang, A.S.; Duan, S.S.; Kang, L.F. Patterns of reproductive allocation in *Artemisia halodendron* inhabiting two contrasting habitats. *Acta Oecologica* **2005**, *28*, 57–64. [CrossRef]
97. Luo, Y.; Zhao, X.; Zhou, R.; Zuo, X.; Zhang, J.; Li, Y. Physiological acclimation of two psammophytes to repeated soil drought and rewatering. *Acta Physiol. Plant* **2011**, *33*, 79–91. [CrossRef]
98. Kim, E.K. Flora and Soil Characteristics on the Reclaimed Tidal Flats in the West Coast of Korea. Ph.D. Thesis, Yonsei University, Seoul, Korea, 2005. (In Korean with English abstract).
99. Oh, W.Y.; Choi, B.K. *Eco-Friendly Restoration of Coastal Reclaimed Land*; Landscape Architecture: Korea, Seoul, 2001; p. 108. (In Korean)